

University of South Bohemia in České Budějovice

Faculty of Sciences

Analysis of trypsin inhibitor-like cysteine-rich domain-containing peptides (TIL-domain inhibitors) from the tick *Ixodes ricinus*

Master thesis

Hana Pechová Bc., BSc

Supervisor: Jan Kotál, Mgr.

Co-supervisor: Jindřich Chmelař, RNDr., Ph.D.

České Budějovice 2020

Pechová H., 2020: Analysis of trypsin inhibitor-like cysteine-rich domain-containing peptides (TIL-domain inhibitors) from the tick *Ixodes ricinus*. Mgr. Thesis, in English – 93 p., Faculty of Science, University of South Bohemia, České Budějovice, Czech Republic.

Annotation:

The master thesis deals with the analysis of trypsin inhibitor-like cysteine-rich domain-containing peptides (TIL-domain inhibitors) extracted from salivary glands of a tick *Ixodes ricinus*. It comprises the initial bioinformatical analysis of TIL-domain containing peptide family from *I. ricinus*, molecular cloning of the representative protein into expression vector, followed by production of recombinant TIL-domain inhibitor in bacteria. A representative TIL-domain gene is proved for their structure, biochemical properties as well as immunomodulatory and anticoagulation features.

I hereby declare that I have worked on my diploma thesis independently and used only the sources listed in the bibliography. I hereby declare that, in accordance with Article 47b of Act No. 111/1998 in the valid wording, I agree with the publication of my master thesis, in full form to be kept in the Faculty of Science archive, in electronic form in a publicly accessible part of the IS STAG database operated by the University of South Bohemia in České Budějovice accessible through its web pages. Further, I agree to the electronic publication of the comments of my supervisor and thesis opponents and the record of the proceedings and results of the thesis defence in accordance with aforementioned Act No. 111/1998. I also agree to the comparison of the text of my thesis with the Theses.cz thesis database operated by the National Registry of University Theses and a plagiarism detection system.

České Budějovice, 9.12.2020

.....

Hana Pechová

Acknowledgments:

I would like to immensely thank my supervisor, Mgr. Jan Kotál. During the whole diploma work, he gave me lots of valuable advice. He always stayed positive, honest, and even when he seemed most unavailable, he was ready to help me, especially when both of us were finishing our studies. I am thankful to know this inspiring, bold, young man.

I would also like to thank my second supervisor, RNDr. Jindřich Chmelař, Ph.D. I am thankful to him that he assigned me with this interesting topic in a progressive working environment and that the work always made sense to me. He was supportive, considerate, and though he is one of the busiest men on the faculty, he was never hesitating to help.

I want to thank my lab colleagues, such as Mgr. Makušová, Mgr. Beránková, Mgr. Chlastáková and others for valuable information based on their rich lab experiences.

The greatest thanks go to my family that was always in all of this with me.

1	Introduction	1
1.1	Proteases	1
1.2	Serine proteases	2
1.3	Malfunctioning serine proteases	2
1.3.1	Artificially synthesized serine protease inhibitors.....	3
1.3.2	Naturally occurring serine protease inhibitors.....	4
1.4	Ticks.....	5
1.5	Serine protease inhibitors in ticks	6
1.5.1	Kunitz-domain inhibitors.....	9
1.5.2	Kazal-domain inhibitors	11
1.5.3	Serpins	12
1.5.4	TIL-domain inhibitors	15
2	Aims	18
3	Materials and methods	19
3.1	Materials	19
3.2	Methods	21
3.2.1	Bioinformatics of TIL-domain family	21
3.2.2	Protein structure prediction	21
3.2.2.1	Swiss model.....	22
3.2.2.2	LOMETS.....	22
3.2.3	Primer design.....	23
3.2.4	Cloning of TIL-1	23
3.2.5	Pilot expression of TIL-1 protein	25
3.2.6	Western blotting	28
3.2.7	Cell disruption	29
3.2.8	Protein purification.....	29

3.2.9	Coagulation assays	29
3.2.9.1	aPTT	30
3.2.9.1	PT	30
3.2.9.2	TT	30
3.2.10	Thrombin assay	30
3.2.11	Trypsin assay	31
3.2.12	LPS decontamination.....	31
3.2.13	Immunologic assays	31
3.2.13.1	Isolation of monocytes	31
3.2.13.2	Monocyte adhesion	32
3.2.14	Expression profile of TIL-1	33
4	Results	35
4.1	Bioinformatics of TIL-domain inhibitors of <i>I. ricinus</i>	35
4.2	Protein structure prediction.....	36
4.2.1	Swiss Model output	36
4.2.2	LOMETS	40
4.2.3	Comparison of predicted structures.....	41
4.3	Preparation of TIL-1 protein.....	42
4.3.1	Transformation of a plasmid into <i>E. coli</i>	43
4.3.2	Pilot expression of TIL-1 protein	44
4.3.3	Western blotting	45
4.3.4	Affinity chromatography	46
4.4	Coagulation assays.....	49
4.4.1	aPTT	50
4.4.2	PT	51

4.4.3	TT	52
4.5	Thrombin assay	53
4.6	Trypsin assay	54
4.7	Purification of TIL-1 inhibitor from LPS	55
4.8	Monocyte adhesion	56
4.9	qPCR.....	58
5	Discussion	59
6	Conclusion.....	64
7	References	65
8	Supplement.....	83

List of abbreviations

AcVSPI	<i>Apis cerana</i> venom serine protease inhibitor
AMCI-1	<i>Apis mellifera</i> cathepsin G/chymotrypsin inhibitor-1
aPTT	Activated Partial Thromboplastine Time
ARDS	Acute respiratory distress syndrome
BCA	Bicinchoninic acid
BmSIs	<i>Rhipicephalus (Boophilus) microplus</i> subtilisin inhibitors
BmSPIs	<i>Rhipicephalus (Boophilus) microplus</i> serine protease inhibitor
Boc-VPR-AMC	Boc-Val-Pro-Arg-7-amido-4-methylcoumarin hydrochloride
BPTI	Bovine pancreatic trypsin inhibitor
BSA	Buried surface area
BSA	Bovine serum albumin
BSTI	<i>Bombina</i> skin trypsin/thrombin inhibitor
C/E-1	<i>Ascaris</i> chymotrypsin/elastase inhibitor-1
CBB	Coomassie Brilliant Blue
cDNA	Complementary DNA
COPD	Chronic obstructive pulmonary disease
Cq	Quantification cycle
CTRL	Control
DNA	Deoxyribonucleic acid
DTT	Dithiothreitol
EF-1	Elongation factor-1
EGF	Epidermal growth factor
FPI-F	Fungal protease inhibitor in <i>Bombyx mori</i>
FWD	Forward
GMQE	Global Model Quality Estimation
HCV	Hepacivirus C
His	Histidine
HIV	Human immunodeficiency virus

hNE	Human neutrophil elastase
IBD	Inflammatory bowel disease
IDT	Integrated DNA Technologies
IL-6	Interleukin 6
IPTG	Isopropyl thiogalactoside
IRIS	<i>Ixodes ricinus</i> immunosuppressor
IRS-2	<i>Ixodes ricinus</i> serpin-2
IRS-8	<i>Ixodes ricinus</i> serpin-8
JAK/STAT3	Janus kinases/signal transducer and activator of transcription proteins
Kan	Kanamycin
LB	Luria broth
LD	Loading dye
LOMETS	Local Meta- Threading-Server
LPS	Lipopolysaccharide
ML	Maximum Likelihood
NNI	Nearest-Neighbor-Interchange
O/N	Overnight
OD	Optical density
PBS	Phosphate-buffered saline
PCR	Polymerase chain reaction
PDB	Protein Data Bank
pET-SUMO	Protein expression system-SUMO
PMA	Phorbol 12-myristate 13-acetate
Pr1	Pr1 protease from <i>Metarhizium anisopliae</i> entomopathogenic fungus
PT	Prothrombin Time
QMEAN	Qualitative Model Energy Analysis
qPCR	Quantitative PCR
rBmTI-A	Recombinant <i>Rhipicephalus (Boophilus) microplus</i> trypsin inhibitor-A
RCL	Reactive-center loop
REV	Reverse

RFU	Relative fluorescence units
RMPI	Roswell Park Memorial Institute
RNA	Ribonucleic acid
rpm	Revolutions per minute
RT	Room temperature
SAT	Saliva assisted/activated transmission
SDS-PAGE	Sodium dodecyl sulphate polyacrylamide gel electrophoresis
serpin	Serine protease inhibitor
SNT	Supernatant
SOC	Super optimal broth
SUMO	Small ubiquitin-related modifier
TBLASTN	Translated nucleotide Basic local alignment search tool
TF	Tissue factor
Th	T helper cells
TIL-domain peptides	Trypsin inhibitor-like cysteine-rich domain-containing peptides
TLR	Toll-like receptor
TSA	Transcriptome Shotgun Assembly
TT	Thrombin Time
ULP1	Ubiquitin-like-specific protease 1

1 Introduction

1.1 Proteases

In biochemical processes such as protein degradation, cellular digestion, and proteolysis, proteins are cleaved to smaller peptides and amino acids by enzymes known as proteases (also called peptidases or proteinases). These enzymes catalyze the hydrolysis of peptide bonds between individual amino acids. In the hydrolysis of proteins and peptides, the structure of the targeted molecule, as well as the active site of protease, play pivotal roles. The surface of protease exposes a catalytic center that is indicated as the 'subsite'. The subsites are numbered as S_1 - S_n to $S_{1'}$ - $S_{n'}$ (cleavage site of the N-terminus towards the C-terminus of the substrate) and the corresponding substrate residues as P_1 - P_n and $P_{1'}$ - $P_{n'}$, respectively (Page and Di Cera, 2008; Schechter and Berger, 1967; Hedstrom 2002). The binding of the substrate towards the active site of the protease is highly specific. Hence, only a particular substrate can be recognized by the corresponding substrate-binding pocket of the enzyme in the key and the lock principle.

Besides the protein degradation role, proteolysis serves as an essential regulatory process in gene transcription, cell-cycle progression, organ formation, homeostasis maintenance, and circadian rhythms (Turk et al., 2006). Protein degradation is also involved in eliminating mutated, non-functional, or aberrantly folded proteins in cells. Simultaneously, proteolysis regulation is needed in an inflammatory response, blood coagulation, tumor suppression, cholesterol metabolism, etc.

The activities of proteases in organisms are controlled at several levels. First of all, proteases are expressed only if required (control at the transcriptional level) (Costantino et al., 2009). They can be expressed either in an active state or in inactive precursors species, alternatively as zymogens that upon activation release mature enzymes (Khan and James, 1998; Ra and Parks, 2007). Secondly, other post-translational modifications are deemed as a control mechanism of proteases, such as phosphorylation (Allan and Clarke, 2009), binding of co-factors (Page and Di Cera, 2008), substrate segregation into vesicles or granules (Cuervo and Dice, 1998; Korkmaz et al., 2008).

The proteases are divided according to their cleavage site (i.e., amino acid involved in the nucleophilic attack) into six categories: serine proteases, threonine proteases, cysteine proteases, aspartyl proteases, glutamyl proteases, and metalloproteases (López-Otín and Bond, 2008).

1.2 Serine proteases

Serine proteases are represented by trypsin, chymotrypsin, elastase, and many more. Therefore, based on substrate specificity, serine proteases can be classified into types such as trypsin-like, chymotrypsin-like, elastase-like, etc. (Blisnick et al., 2017). They bind substrates with highly reactive serine (acts as a nucleophile) residue together with neighboring histidine, and aspartate forming a catalytic triad. However, the sequence specificity of the serine proteases differs, i.e., trypsin cleaves after positively charged amino acids (lysine or arginine), chymotrypsin mainly after aromatic amino acids (on the carboxyl residue of phenylalanine, tyrosine, or tryptophan), and elastase prefers small amino acids like alanine, glycine, valine, or serine.

Serine proteases occur in numerous isoforms and homologs in eukaryotes, prokaryotes, viruses, and archaea (Irving et al., 2000; Tripathi and Sowdhamini, 2008; Patel 2017). Among other manifestations, serine proteases are building blocks of coagulation cascade and complement. Tick, being a hematophagous ectoparasite, can suppress the host serine proteases in order to inhibit the coagulation and complement activation. Hence, serine proteases are worth investigating in the role of tick-host interaction (Chmelar et al., 2012, 2017, 2019; Blisnick et al., 2017).

1.3 Malfunctioning serine proteases

Despite a strict control on the transcriptional level, serine proteases often participate in pathological processes. Several studies bring evidence for the connection between malfunctioning or suppressed serine proteases and serious diseases such as arthritis, cystic fibrosis, atherosclerosis, cancer, and many more. (Miyata et al., 2007; Han et al., 2011; Lima and Monteiro, 2013; Sandhaus and Turino, 2013). Furthermore, serine protease-associated disorders affect the gastrointestinal tract causing inflammatory bowel disease (IBD), including gastritis, esophagitis, and severe ailments like Crohn's disease and ulcerative colitis (Vergnolle, 2016; Ceuleers et al., 2018).

The recent reviews dealing with the serine proteases, namely kallikreins, kallikrein-related peptidases, neutrophil elastases, and plasmin, have attracted the most significant interest in the development of their inhibitors in recent years. Mentioned proteases are mainly associated with

skin diseases like psoriasis or atopic dermatitis (De Veer et al., 2014; Zhu et al., 2017). Moreover, these skin disorders have been shown to cause chronic systemic health ailments such as diabetes, allergic and cardiovascular diseases (Guttman-Yassky et al., 2017). Apart from the skin disorders, lung inflammation (such as pneumonia, asthma, acute respiratory distress syndrome (ARDS) and chronic obstructive pulmonary disease (COPD)) are globally spread illnesses affecting and killing millions of people every year worldwide (Kettritz, 2016; Eapen et al., 2017).

Therefore, malfunctioning proteases are critical signaling molecules in diagnostics, and they have been characterized in numerous publications to specify functional protease inhibitors (Drag and Salvesen, 2010; Turk 2006; Palermo and Joyce, 2008; Quinn et al., 2010; Caughey 2016).

1.3.1 Artificially synthesized serine protease inhibitors

The artificial protease inhibitor development's relied strategy is to synthesize an analogous substrate that would compete in the active site and block the regular substrate binding (Turk, 2006). For this purpose, one must precisely characterize the enzyme active site's structure to ensure high specificity and efficacy of that substrate analog binding (binding of the inhibitor) (Pirard, 2007).

Nevertheless, optimizations of a large set of inhibitors remain to be performed. Bringing such protease inhibitors on the market must be based on exact knowledge of their substrate processing as well as finding the appropriate balance in modifying the protease activity (Liang and Bowen, 2016). The way of action of the inhibitors must not cause damaging side effects. Similarly, the thermodynamic and chemical properties of the drug (i.e., reversibility of the reaction through creating non-covalent complexes or transient states) shall lead to an effective inhibitor reactivation (Krantz, 1992; Soualmia and El Amri, 2017).

Almost a hundred artificially synthesized serine protease inhibitors have undergone clinical trials for different indications, e.g., Apixaban by Bristol-Myers Squibb (an antithrombotic agent), Sivelestat, and Camostat by Ono Pharmaceutical (a competitive inhibitor of neutrophil elastase and proteolytic enzyme inhibitor resp.). The artificially synthesized serine protease inhibitors are widely used mostly as antiviral drugs, e.g., atazanavir (human immunodeficiency virus HIV-

protease inhibitor), simeprevir (hepacivirus C HCV-protease inhibitor), nafamostat (analgesics in cystic fibrosis), etc. (source: <http://drugcentral.org>).

However, the most efficient serine protease inhibitors were inspired by the peptide-based or peptidomimetic inhibitors, especially those present in nature.

1.3.2 Naturally occurring serine protease inhibitors

Both serine proteases and serine protease inhibitors are ubiquitously present in organisms. Both of them are connected like two sides of the same coin. Serine protease inhibitors represent the most diverse and numerous protease inhibitors that are abundant in all eukaryotes (Irving et al., 2000; Silverman et al., 2001). Their role in organisms is to control the serine proteases that take part in crucial biological processes, like fibrinolysis, hemostasis, apoptosis, complement activation, inflammation, etc.

The naturally occurring inhibitors of serine proteases can be divided into several families isolated from different organisms. The bacteria producing serine protease inhibitors include pepstatin originally isolated from actinomycetes (Umezawa et al., 1970). A rich source of serine protease inhibitors are plants. They defend against herbivorous animals using the inhibitors (Hartl et al., 2011), represented by, e.g., lima bean trypsin inhibitor (Haynes and Feeney, 1967), soybean Bowman-Birk inhibitors (Birk et al., 1967), mushroom-produced aprotinin (Zheng et al., 2011). In response to serine protease inhibitors in plants, a plant-parasitic moth *Helicoverpa armingera* has even evolved a serine protease that is protease inhibitor-resistant (Kuwar et al., 2015). High levels of ovomucoid serine protease inhibitors are produced by chickens and turkeys (Lineweaver and Murray, 1947). Well-studied Kunitz-domain inhibitors are present mostly in venoms of spiders, ticks, snakes (Wan et al., 2013; Chmelar et al., 2012; Liu et al., 2015). Kazal-domain inhibitors are widely recognized in viruses, fungi, termites, mice, helminths, jellyfish, echinoderm sea cucumber, and humans (Ohmuraya and Yamamura, 2011; Molehin et al., 2012; Negulescu et al., 2015; Jouiaei et al., 2015; Murakami et al., 2012).

As previously said, serine protease inhibitors are present in animals, plants, even in certain viruses, bacteria, and archaea (Irving et al., 2000). Nevertheless, especially promising sources of

naturally abundant serine protease inhibitors are ticks and other blood-feeding parasites, with their salivary glands in particular.

1.4 Ticks

Ticks are ectoparasitic hematophagous arthropods that secrete saliva into the host to suppress the immune reaction and successfully feed on the host. Ticks are classified into three families; soft ticks (*Argasidae*), hard ticks (*Ixodidae*), and *Nuttalliellidae*. Soft ticks can sufficiently feed on the host within 1 hour (Sonenshine and Anderson, 2014), whereas hard ticks need several days to satiate. When a tick bites a host, it inserts its hypostome into the wound and injects saliva (see Figure 1). Saliva is full of pharmacologically active components (mostly proteins) with anti-hemostatic, anti-inflammatory, anti-complement properties that modulate the host defense mechanisms. Ticks developed these immunomodulatory mechanisms to overcome the host immune systems in order to thrive and develop successfully (Brossard and Wikel, 2004; Chmelar et al., 2012).

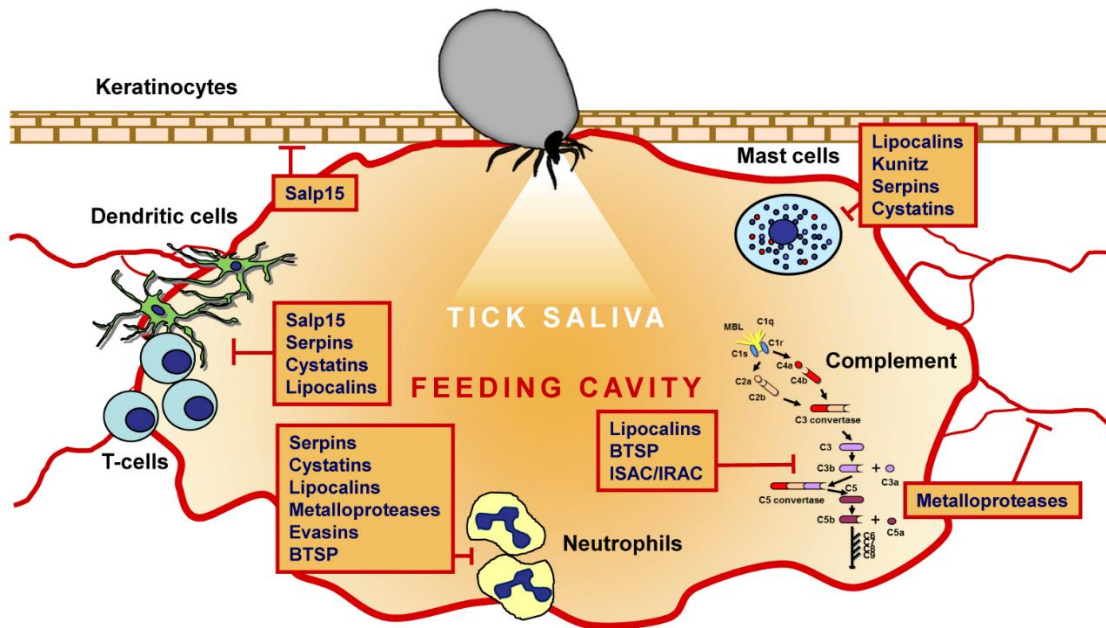


Figure 1: Major protein families secreted into the feeding cavity of tick at the bite location and inhibition of processes responsible for an anti-tick immune response (Chmelar et al., 2019).

Immunomodulatory components present in tick saliva seem redundant and pluripotent. Different inhibitors can cause a similar effect in the host metabolism by targeting different pathways or by

targeting other triggers in one pathway. Moreover, one inhibitor can cause more than one effect. This fact can be interpreted as the long-term tick-host coevolution (Chmelar et al., 2016).

While feeding, ticks can transmit a variety of pathogens. Bacterial pathogens are represented by the genera *Anaplasma*, *Borrelia*, *Rickettsia*, *Francisella*, and others. *Borrelia burgdorferi* from *Borrelia* genera is causing Lyme disease, also known as borreliosis (Ramamoorthi et al., 2005; Russell et al., 2018). Besides bacteria, ticks can also transfer protozoan parasites (from *Babesia* and *Theileria* genus) and viruses (families *Asfarviridae*, *Reoviridae*, *Rhabdoviridae*, *Orthomyxoviridae*, *Bunyaviridae*, and others). Tick-borne encephalitis virus from the *Flaviviridae* family causes tick-borne encephalitis, the most threatening human virus transmitted by ticks (Swanson et al., 2006; Kazimirova et al., 2017; Dehghani et al., 2019).

Several publications have described tick saliva produced by salivary glands as the key factor in tick-host-pathogen interaction. The effect is called saliva assisted/activated transmission (SAT) (Nuttal and Labuda, 2004, 2008). A recent publication by Pospisilova and collective evidence that saliva is not necessarily needed for successful pathogen transmission, although the benefits of saliva pharmacologically active components are nonnegligible (Pospisilova et al., 2019). Nevertheless, when these salivary components are studied from the medicinal perspective, they can show us the potential to become effective drugs in treating many human deficiencies (Chmelar et al., 2017; Blisnick et al., 2017; Florencio et al., 2019).

1.5 Serine protease inhibitors in ticks

The serine protease inhibitors isolated from ticks can be divided based on their inhibitory mechanism into two kinds: tight-binding and trapping inhibitors (Blisnick et al., 2017). Tight-binding inhibitors (Kunitz or Kazal domain-containing peptides) possess conserved domain(s). Together with the protease remain in the same undamaged structure upon splitting of the inhibitor-protease complex. On the other hand, trapping inhibitors (serpins) are characterized by inhibition by deformation owing to their specific “suicide substrate-like inhibitory mechanism” (Huntington et al., 2000; Silverman et al., 2001). Huntington and collective studied the inhibition of a typical serpin present in human plasma, α_1 -antitrypsin (Huntington et al., 2000). The structure of the α_1 -antitrypsin-trypsin complex was observed by x-ray crystallography. The serine protease (trypsin)

thereby cleaves the reactive-center loop (RCL) of the serpin at “scissile bond” (P1-P1’) and creates a noncovalent Michaelis-like complex. The cleaved RCL can be shifted together with the protease to the opposite site of the serpin. This tight enzyme-inhibitor linkage causes the inactivation by modifying the enzyme structure that prevents the protease from being released from the complex (a covalent complex). The successful creation of the serpin-protease complex is due to the irreversibility and long-lasting stability of the complex (Olson et al., 1995). Alternatively, once serpin altered its structure, the active site is distorted. The protease can be slowly dissociated by hydrolysis of acyl bonds while cleaving and inserting RCL into serpin’s central β -folded sheet (Gettins, 2000; Huntington et al., 2000; Silverman et al., 2001). Simultaneously, protease can be pointed towards proteolysis (Huber and Bode; 1978, Bode and Huber 2000; Kaslik et al., 1995). The fate of serpin and protease is depicted in Figure 2.

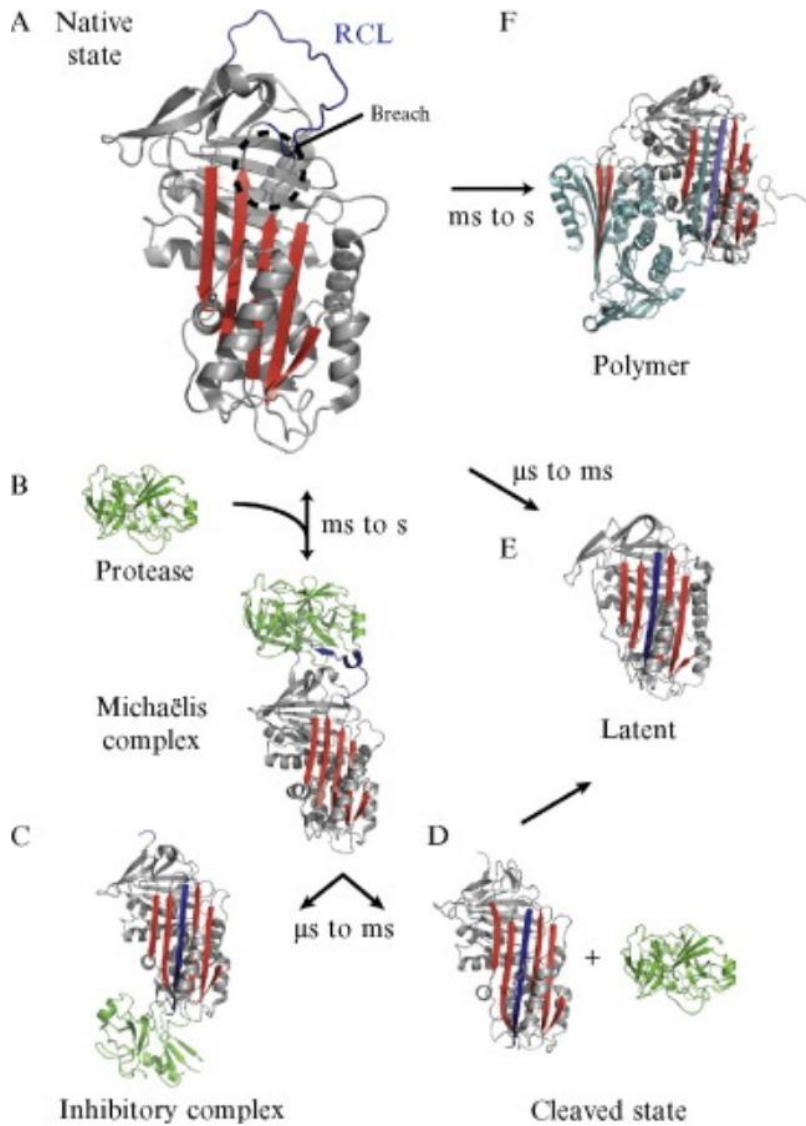


Figure 2: Mechanism of serpin-protease inhibition. A) Native state active serpin exposes RCL. B) Free protease binds to the RCL of the serpin, creating a noncovalent Michaelis complex. C) After cleaving RCL at “scissile bond”, the protease is mechanically modified by shifting towards the opposite pole of the serpin, where it either remains and creates an inhibitory covalent complex (suicide inhibition) or D) the protease cleaves the serpin without being inhibited and E) serpin is made inactive (latent). F) Alternatively, native serpin can create polymers. Modified from Kass et al., 2011.

Moreover, the mechanism of serpin's nonspecific inhibition with its RCL explains the pluripotent effect on several serine proteases (Huntington et al., 2000). Yet, the length and activity of the RCL seem crucial in the (ir)reversibility aspect. When, for example, RCL was impeded, the protease escaped from the serpin complexation, so the protease remains active, and the serpin was deactivated (Gettins et al., 1996). Similarly, if the serpin was bound to specific pentasaccharide heparin, the resulting affinity of the serpin-protease complex was increased by 1000-fold (Johnson and Huntington, 2003).

With the possibility of proteomics studies of tick saliva and transcriptomics of tick salivary glands, tens of protein families have been identified in the last decade (Tirloni et al., 2014, 2015, 2017; Kotsyfakis et al., 2015a, b; Ribeiro et al., 2017; Perner et al., 2016a, 2018; Giachetto et al., 2020). In salivary glands of *Ixodes ricinus*, four groups of serine protease inhibitors have been described. These are Kunitz domain inhibitors, Kazal domain inhibitors, serpins, and trypsin inhibitor-like cysteine-rich domain (TIL) inhibitors. Specifications and functions of the mentioned four groups are discussed further in detail.

1.5.1 Kunitz-domain inhibitors

One group of the serine proteases inhibitors widely present in nature are Kunitz domain inhibitors, also called BPTI (refers to the most well examined bovine pancreatic trypsin inhibitor). These proteins were first discovered in soybeans (Kunitz, 1945). These inhibitors contain one to twelve Kunitz domains where one domain can have a molecular weight of about 7 kDa and forms a rigid structure. Thanks to their tight-binding reversible mechanism, the protease dissociates from the complex unchanged, as mentioned above. Kunitz-domain is composed of disulfide-rich α -helices and β -sheets strengthened by three disulfide bridges (Ranasinghe and McManus, 2013). Proteins belonging to the Kunitz domain include, e.g., aprotinin (bovine pancreatic trypsin inhibitor), that inhibits plasmin, trypsin, and kallikrein and is commonly used in antifibrinolytic therapy (Waxler and Rabito, 2003; Scott and Taggart, 2010). Neutrophil elastase inhibitor, mostly in cardiopulmonary pathologies, belongs to the Kunitz proteins (Crocetti et al., 2019). Kunitz family is one of the largest groups of proteins present in tick saliva, where most of the characterized Kunitz-domain protease inhibitors were proved to counteract the coagulation cascade in several steps (Maritz-Olivier et al., 2007; Corral-Rodriguez et al., 2009; Chmelar et al., 2012, 2019).

Lately, recombinant Kunitz-domain inhibitor rBmTI-A (recombinant *Rhipicephalus (Boophilus) microplus* trypsin inhibitor) was tested for its putative anti-inflammatory properties in mice with chronic allergic lung inflammation (Florencio et al., 2019). The study confirmed that the rBmTI-A attenuated bronchial hyperresponsiveness, inflammation. Hence, it proved itself a potential therapeutic tool in asthma treatment (Florencio et al., 2019). Another recent study revealed quelling of emphysema in mice exposed to cigarette smoke by nasal administration of rBmTI-A (Lourenço et al., 2018)

A representative of Kunitz-domain inhibitors isolated from tick *Ixodes scapularis* is Ixolaris. The structure creates an inhibitory complex that possesses two Kunitz domains (rigid K1 domain and dynamic K2 domain) (see Figure 3). The protease inhibitor makes a tight complex with coagulation factor Xa outside its active site; hence it interacts noncanonically via salt bridge formation. Ixolaris is an important regulator of factor Xa of the coagulation cascade (Francischetti et al., 2002; Grover and Mackman, 2018; De Paula et al., 2019).

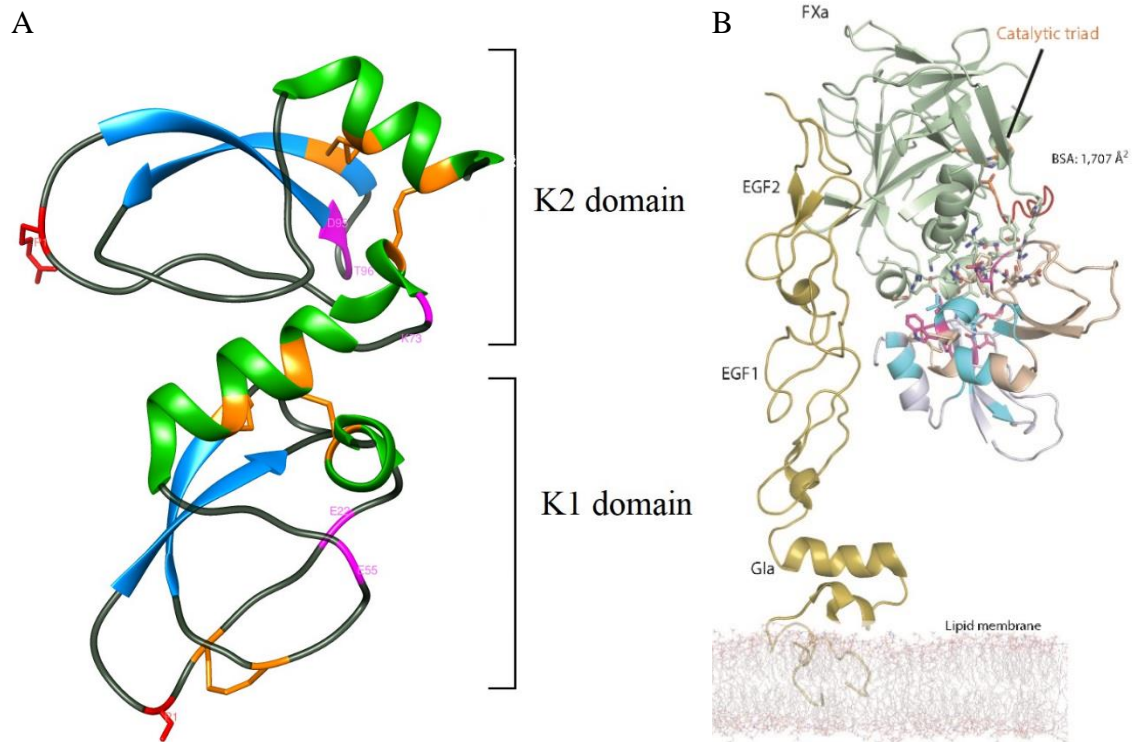


Figure 3: Structure of the Ixolaris with the K1 and K2 domains as the representative of Kunitz domain inhibitors. A) α -helices colored in green, β -sheets in blue, the coil in grey, cysteines with

5 disulfide bridges in orange, the active sites of each domain P1 colored in red at Ser28 on K1 and Arg86 on K2 domain, interacting sites (Glu22, Glu55, Lys73, D95, and Thr96) of Ixolaris with factor X in magenta (PDB accession code 6NAN). B) Tight complex of coagulation factor Xa (FXa) shown as green ribbon and Ixolaris with K2 domain as light blue and K1 complexed with the FXa as wheat ribbon interacting via the pink salt bridge. It is shown the orientation of membrane-associated FXa by the EGF (epidermal growth factor) and Gla (glutamate residues) domains. The FXa catalytic triad is shown as orange sticks (BSA-buried surface area) (De Paula et al. 2019).

Besides the regulation of homeostasis, Ixolaris prevents thrombosis (Nazareth et al., 2006), tumor growth (Versteeg et al., 2008; Ruf, 2012), and it blocks immune activation observed in HIV positive patients in particular (Schechter et al., 2017).

1.5.2 Kazal-domain inhibitors

Kazal-domain inhibitors are another group of serine protease inhibitors that have a highly conserved cysteine-rich structure. They were first recognized as trypsin inhibitor-anticoagulant proteins in the porcine pancreas (Kazal et al., 1948). One inhibitor can consist of 2 to 15 of Kazal domains (Rawlings et al., 2004), each composed of one α -helix and three β -sheets and loops (Cerenius et al., 2010; Rimphanitchayakit and Tassanakajon, 2010). With the help of exposed RCL, Kazal inhibitors create a stable inhibitor-protease complex. Moreover, the noncovalent tight complex binding provides potent inhibition (Somprasong et al., 2006; Wang et al., 2009). The length of RCLs differentiates Kazal-domain inhibitors into diverse groups, i.e., inhibitors found in vertebrates and invertebrates. This group of inhibitors can suppress trypsin, plasmin, human neutrophil elastase (hNE), chymotrypsin, proteinase K, and thrombin (Rimphanitchayakit and Tassanakajon, 2010). Furthermore, in hematophagous animals such as leech, mosquitoes, and ticks, Kazal-domain inhibitors are secreted to act as anticoagulants. They can also defend the parasite from microbial proteinases or the host digestive proteases. In Figure 4, we can see Dipetalin (Schlott et al., 2002), a Kazal-domain inhibitor representative with only one domain isolated from blood-sucking insect *Dipetalogaster maximus*, also known as kissing bug. The inhibitory protein obtained from this bug showed interaction with thrombin and trypsin (Schlott et al., 2002).

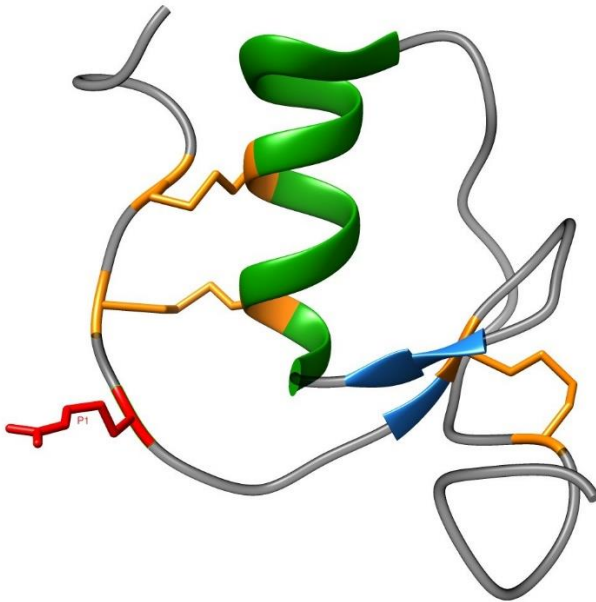


Figure 4: Structure of Dipetalin as the representative of Kazal-domain inhibitors with one Kazal domain. One α -helix is colored in green, two short β -sheets in blue, the coil in grey, 6 cysteines with 3 disulfide bridges in orange, the active site P1 at Arg10 is red (PDB accession code: 1KMA).

The predominating structures of Kazal domain-containing inhibitors accessible on Protein Data Bank (PDB) are from humans, pigs, and insects like mosquitoes. Structural studies in this direction might appear promising when targeting Kazal-domain inhibitors extracted from tick saliva.

1.5.3 Serpins

Serine protease inhibitors from ticks (serpins) are the most abundant and numerous superfamily of protease inhibitors. The superfamily grew up based on similarities in primary structures of ovalbumin, α_1 -antitrypsin, and human antithrombin (Hunt and Dayhoff, 1980; Carrel and Travis, 1985). Mostly they consist out of 400 amino acids that occur in glycosylated forms. The structural arrangement of serpins is unobviously distinct from those of Kunitz-, Kazal- or TIL-domain inhibitors. Serpins usually possess 3 β sheets, 8-9 α helical linkers, and up to 20 residues long RCL (Hunt and Dayhoff, 1980; Gettins et al., 1996). Unlike other serine protease inhibitors, serpins do not contain any conserved cysteine core, making their native fold highly unstable (Law

et al., 2006). The intriguing mechanism of inhibition supports this fact, which was generally described above in Chapter 1.5. Serpins are so-called trapping inhibitors, which means that RCL is cleaved after proteolysis. The terminal portion, thereby, covalently binds the protease molecule and is spontaneously inserted into the β -sheet A center. Protease is, therefore, inactivated and, as a consequence, the serpin-protease complex is degraded (Huntington et al., 2000; Law et al., 2006; Huntington and Li, 2009). They preferably suppress the activity of serine proteases; however, serpins bind to the active center of many other proteases too. These include cysteine proteases, metalloproteases, caspases, papain-like cysteine proteases (Irving et al., 2000). The reactivity was shown with ligands such as collagen, DNA, heparin, or heparin sulfate co-factor. Serpins can even act as non-inhibitory molecules and are known as hormone transporters (Pemberton et al., 1988; Carrel and Read, 2016), chaperons (Nagata, 1996), or tumor suppressors (Zou et al., 1994).

The coagulation cascade is assembled from serine proteases. Similarly, in immune response, complement is activated by serine proteases. Serpins, being serine protease inhibitors, affect each step of the coagulation cascade. Thus, their predominant function is to modulate hemostasis and complement (Kanost, 1999; Colinet et al., 2009; Calvo et al., 2011). Similarly, malfunctioning serpins are related to emphysema, cirrhosis, angioedema, hypertension, and familial dementia (Kim et al.; 1995; Davis et al., 1999; Huntington and Li, 2009; Lomas et al., 2016).

Recently, a high number of tick transcriptomic studies broadened the number of inhibitors belonging to the serpin family (Schwarz et al., 2013; Kotsyfakis et al., 2015a, b; Perner et al., 2016a; Giachetto et al., 2020). Many of them were characterized functionally, yet the majority of serpins remains to be analyzed deeper.

As the representative of the serpin family, IRS-2 (*Ixodes ricinus* serpin-2) can be mentioned and is as shown in Figure 5 below.

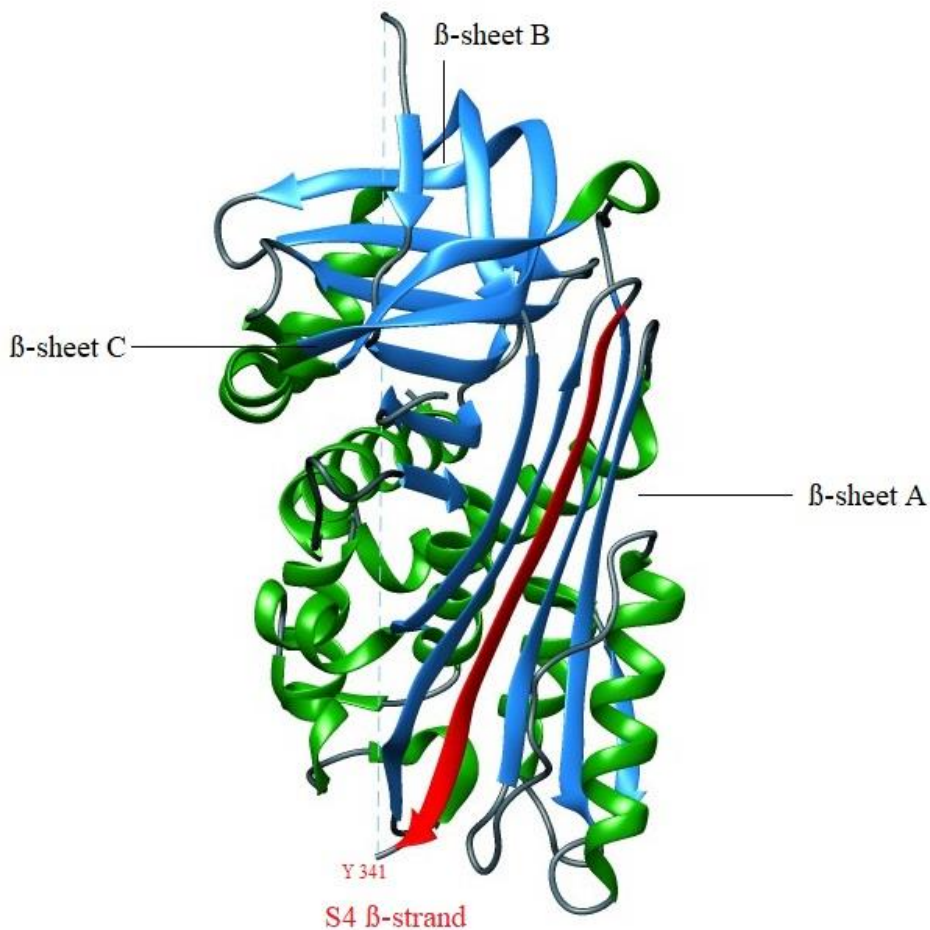


Figure 5: Structure of IRS-2 composed of 9 α -helices colored in green, 3 large β -sheets in blue, coil colored in grey. Since the structure resembles serpin in its relaxed state (R-state), RCL was cleaved at residue Tyr341 (P1) and inserted into the β -sheet A as a S4 β -strand (PDB accession code: 3NDA)

It is the second serpin characterized from *I. ricinus* (Kovarova et al., 2010; Chmelar et al., 2011) after IRIS – *Ixodes ricinus* immunosuppressor (Leboulle et al., 2002; Prevot et al., 2006). The latter study proved that IRS-2 has anti-inflammatory properties; namely, IRS-2 suppressed the mast cell chymase and cathepsin G. Similarly, IRS-2 inhibited platelet aggregation and restrained neutrophil recruitment and paw swelling in paw edema experiment (Chmelar et al., 2011). Another study revealed that in the inflamed tissues, IRS-2 inhibited cytokine IL-6 by dendritic

cells and so disrupted JAK/STAT3 signaling in T helper (Th) cells as well as the maturation of proinflammatory Th17 lymphocytes (Palenikova et al. 2015).

1.5.4 TIL-domain inhibitors

Trypsin inhibitors- like cysteine-rich (TIL)-domain inhibitors represent an interesting group of small proteins. The tight-binding domain of TIL inhibitors is composed of 10 cysteines forming 5 disulfide bridges with the exposed loop between 5th and 6th cysteine residue that act in different organisms in anticoagulation, self-defense mechanisms, antibacterial and immunomodulatory processes (Bania *et al.*, 1999; Fogaca *et al.*, 2006; Sasaki *et al.*, 2008).

Initially, the TIL domain family was named *Bombyx* family, after the fungal protease inhibitor (FPI-F) found in *Bombyx mori* (Pham et al., 1996). To date, the TIL domain inhibitors have been described in hemocytes of tick species like *Rhipicephalus microplus*, described as Ixodidin (Fogaca *et al.*, 2006) and BmSIs inhibitors (*R. (Boophilus) microplus* subtilisin inhibitors) (Sasaki *et al.*, 2008). Both inhibitors presented the inhibitory activity to serine protease inhibitors (Ixodidin to chymotrypsin and elastase, BmSIs to subtilisin A and hNE). Moreover, TIL-domain inhibitors from *R. microplus* showed growth inhibition of *Escherichia coli* and *Micrococcus luteus* (Fogaca et al., 2006), and they inhibited fungal protease Pr1 (Sasaki et al., 2008).

Besides ticks, the TIL inhibitors have been reported in honeybees *Apis cerana* (named as *Apis cerana* venom serine protease inhibitor, AcVSPI, Yang, et al., 2017) and *Apis mellifera* hemolymph (named as *A. mellifera* cathepsin G/chymotrypsin inhibitor, AMCI-1), latter shown in Figure 6 (Bania *et al.*, 1999; Cierpicki et al., 2000; Michel *et al.*, 2012).

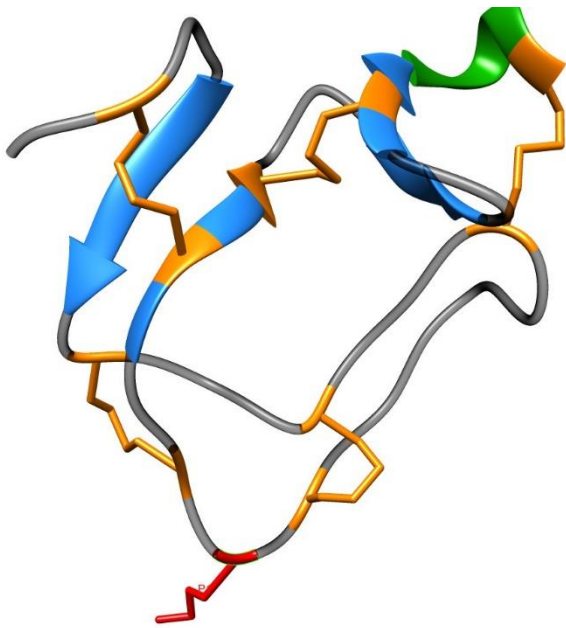


Figure 6: Structure of AMCI-1, a cathepsin G/chymotrypsin inhibitor from *Apis mellifera*. One short α -helix is colored in green, 4 short β -sheets in blue, the coil in grey, 10 cysteines with 5 disulfide bridges in orange, the active site P1 at Met30 is red (PDB accession code: 1CCV).

TIL domain inhibitors were also isolated from silkworm *B. mori* (Pham et al., 1996; Zhao et al., 2012; Li et al., 2015, 2016a, 2018), in parasitoid wasp *Cotesia vestalis* (Gu et al., 2019), in the skin of frogs *Bombina bombina* (Mignogna et al., 1996) and *Lepidobatrachus laevis* (Wang et al., 2015), Chinese scorpion *Mesobuthus martensii* (Zeng, 2014), but also in helminths such as *Ascaris* nematodes called chymotrypsin/elastase inhibitor complex (C/E-1) (Bernard and Peanasky, 1993; Huang et al., 1994). Selected organisms from Arthropoda phylum have been used for genome-wide search and genomic analysis of TIL domain, which showed that TIL domain peptides can be classified into seven evolutionary distinct groups (Zeng et al., 2014).

In comparison to mammals, ticks do not possess lymphocytes or immunoglobulins as a part of their immune system. Instead, serine protease inhibitors play crucial role in tick immunity (Cerenius et al., 2010; Fullaondo et al., 2011; Kanost, 1999; Tang et al., 2008). During microbial pathogen invasion the microorganism proteases enable penetration of host protective barrier e.g. cuticle (Travis et al. 1995). In response to antimicrobial extracellular proteases (especially those of fungal origin), serine protease inhibitors are secreted in large amounts by the tick to suppress

the pathogen proliferation (Augustin et al., 2009; Wang et al., 2009). Therefore, blocking the antimicrobial properties of serine protease inhibitors appears useful in the biological control of insects, especially ticks (Sasaki et al., 2008).

As already mentioned, antifungal properties of serine protease inhibitors were shown for BmSI-7 extracted from tick *R. microplus* (Sasaki et al., 2008). BmSI-7 belonging to TIL domain family exerts inhibition against subtilisin A and Pr1 protease from entomopathogenic fungus *Metarhizum anisopliae* (Sasaki et al., 2008). Another TIL domain inhibitor called *R. (Boophilus) microplus* serine protease inhibitor, BmSPI38 from silkworm *B. mori* is involved in defense against microbial proteases of the entomopathogenic fungus *Beauveria bassiana* (Li et al., 2012b). The antifungal activity of TIL domain peptide inhibitors from *B. mori* was caused mainly by the loss of two cysteines. Upon insertion of Cys2 and Cys6 by site-directed mutagenesis into the proteins BmSPI38 and BmSPI39, the mutated TIL domain peptides' inhibitory activity against microbial proteases was dramatically lowered (Li et al., 2016). Honeybee *A. cerana* venom contains TIL-domain inhibitors (designated as AcVSPI) that showed antifibrinolytic and antimicrobial activities, too (Yang et al., 2017). Hence, this inhibitor group seems to be a promising model for designing novel antimicrobial peptides and serine protease inhibitors (Li et al., 2007).

Salivary glands of *I. ricinus* have so far undergone massive *de novo* sequencing (e.g., Schwarz et al., 2013; Kotsyfakis et al., 2015a, b), RNA sequencing, and comparison of their transcriptomes (Perner et al. 2016a, 2018) and many TIL domain inhibitors were detected. However, TIL domain inhibitors from *I. ricinus* salivary glands have never been investigated further for their putative immunomodulatory, anticoagulation, and other biological properties. Moreover, the phylogenetic analysis of TIL domain inhibitors from wide range of organisms might help to reveal the evolution of this multigenic protein family.

This thesis presents a novel *I. ricinus* TIL-domain inhibitor named TIL-1. I show an *in silico* analysis of the TIL-domain family of *I. ricinus*, cloning, expression and purification of recombinant TIL-1 inhibitor. The TIL-1 inhibitor is tested for its putative anticoagulation and immunomodulatory properties and as a protease inhibitor. The expression profile of TIL-1 in tick tissues is shown in various stages of tick feeding.

2 Aims

- 1) *In silico* analysis of existing TIL-domain inhibitors from *I. ricinus*
- 2) Optimization of conditions for the expression of TIL domain inhibitors
- 3) Expression and purification of the protein
- 4) Study of resulting recombinant protein for its biochemical, immunomodulatory, and anticoagulation properties.
- 5) Expression profile of TIL-1 in tick tissues in various stages of tick feeding

3 Materials and methods

3.1 Materials

A list of used chemicals is summarized in Table 1. Each consumable preparation and manufacturer are described concerning every single procedure. Note that the list does not include the chemicals, those concentrations, manufacturers, and preparations are described in Methods (see later).

Procedure	Chemical	Preparation	Manufacturer
Cloning	1% agarose gel	70 ml of 1x Tris Acetate EDTA (TAE)	Lachner
		0.7 g agarose boiled 1 min in microwave 7 ul of SYBR added into the cooled (but not solidified) solution	Roth Sigma
Protein expression	LB plates	35 g/l of Luria broth with agar (Lennox) autoclave 50 ug/ml Kanamycin	Sigma Sigma
	LB medium	25 g/l of Luria broth (Miller) autoclave 50 ug/ml Kanamycin	Sigma Sigma
	500 mM NaCl- Tris	500 mM NaCl 20 mM Tris pH 8	Penta VWR
	Coomassie Brilliant Blue	1% dissolved in destaining solution	BioRad
	Destaining solution	50% H ₂ O 40% methanol 10% glacial acetic acid	VWR VWR
Affinity chromatography	Buffer A	20 mM Tris 500 mM NaCl	VWR Penta

		pH 8	
	Buffer B	20 mM Tris 500 mM NaCl 500 mM imidazole pH 8	VWR Penta ITW Reagents
Western blot	PBS-Tween	10x PBS stock 0.1% Tween	Penta Sigma
	Blocking solution	3% dried milk in PBS-Tween	Nutristar
Coagulation assays		plasma Coagulation Control N Technoplastin HIS (Ca-thromboplastin) Dapttin 25 mmol/l CaCl ₂ 20 I. U. bov. Trombin (Thrombin Reagent)	Technoclone Technoclone Technoclone Technoclone Technoclone
Anti-protease assays	Thrombin assay	20 mM Tris 150 mM NaCl 5 mM CaCl ₂ 0.2% BSA 0.1% polyethylen glycol (PEG) pH 7.4	VWR Penta Penta Sigma Sigma
	Trypsin assay	50 mM Tris 150 mM NaCl 10 mM CaCl ₂ 0.05% Triton X-100 pH 7.4	VWR VWR Penta Sigma

Table 1: List of used chemicals, preparations, and manufacturers, in each procedure

3.2 Methods

3.2.1 Bioinformatics of TIL-domain family

Prior to laboratory work, I performed deep *in silico* analysis of the TIL-domain protein family. On the National Center for Biotechnology Information website (ncbi.nlm.nih.gov), I searched for “trypsin inhibitor like cysteine-rich domain protein” and “*Ixodes ricinus*” at the same time. I chose representative protein (contains 10 cysteines) with GenBank query ID JAA72280.1. I blasted with this accession number through TBLASTN (Altschul et al., 1997) in Transcriptome Shotgun Assembly (TSA) database with the limited search for *I. ricinus* only. Results of the search offered me 78 similar proteins found in 7 databases based on 7 TSA projects.

I searched for signal segments within these 78 sequences with online server SignalP (<http://www.cbs.dtu.dk/services/SignalP>) (Nielsen et al., 1997). I erased the signaling peptides from the sequences and controlled the correct reading frame using BioEdit Sequence Alignment Editor (version 7.2.6.) (Hall 1999).

Afterward, I searched for phylogenetic clustering to organize selected proteins into groups. To root the phylogenetic tree with an outgroup, I used TBLASTN, where I first included and then excluded Suborder *Ixodida* from the TSA database search. Sequences from both searches, i.e., 194 nucleotide sequences were used for the phylogenetic tree based on Maximum Likelihood (ML) method with the Tamura-Nei model (Tamura and Nei, 1993), Nearest-Neighbor-Interchange (NNI) as the Heuristic method, 1000 Bootstrap Replications and Complete deletion in case of gaps or missing data. I used MEGA software version 7.0.26 (Kumar et al., 2016) for this purpose.

3.2.2 Protein structure prediction

To the best of my knowledge, the TIL-domain protein structure from *I. ricinus* has not been resolved yet. In this thesis's scope, there was not enough time to determine the 3D structure of this protein. Nonetheless, knowing the exact protein structure would help me better understand its putative anticoagulation, immunomodulatory and antimicrobial properties. For TIL-domain protein structure prediction, I used two online servers: Swiss model (<https://swissmodel.expasy.org/>) (Guex et al., 2009; Bienert et al., 2017; Bertoni et al., 2017;

Waterhouse et al., 2018; Studer et al., 2020) and Local Meta- Threading-Server (LOMETS) (<https://zhanglab.ccmb.med.umich.edu/LOMETS/>) (Wu and Zhang 2007; Zheng et al., 2019). As the target sequence, I used TIL-1 protein with its sequence shown below:

ARIAADLPWVCGPREVFKTCVSSSCAELKCGMEGMPEACTMDCASGCFCAPGFYRKG
HRECVPWSECQIEPLKMPKA

All protein structures, including model structures, were edited using UCSF Chimera version 1.8 software (Pettersen et al., 2004).

3.2.2.1 Swiss model

The Swiss model template library searches with BLAST+ (Camacho et al. 2009) and HHBlits (Steinegger et al., 2019) for evolutionary related structures matching the target sequence. In the Swiss model server, I entered the sequence of selected TIL-1 protein and searched for the most similar proteins with resolved structures. Based on the existing determined TIL-domain protein structures, the Swiss model created several predictions of TIL-1 protein based on two different scores of reliability in terms of quality estimation: Global Model Quality Estimation (GMQE) (Waterhouse et al., 2018) and Qualitative Model Energy Analysis (QMEAN) (Benkert et al., 2011; Studer et al., 2020). GMQE score moves between 0 and 1; the higher GMQE, the higher the reliability. The quality estimation is increased when GMQE is combined with QMEAN. The latter score represents the global (the whole structure) and local (per-residue) model quality estimation. The QMEAN value around zero validates high similarity between the model and experimental protein structure. On the contrary, models with QMEAN scores around and lower than -4 should not be considered for their low quality and small reliability (Benkert et al., 2011).

3.2.2.2 LOMETS

With the help of LOMETS, the structure of the desired protein was predicted based on ranking and selecting high-scoring structural templates. I entered the TIL-1 sequence to LOMETS, and iterative sequence homology searches generated deep multiple sequence alignments through 11 individual threading programs. The advantage of using LOMETS is that the quality of models predicted is relatively high. Moreover, it possesses the user information of the target protein, such

as the protein function based on the simultaneous deep search of multiple protein databases. Several scores then ranked the predicted structures (Wu and Zhang, 2007; Zheng et al., 2019).

3.2.3 Primer design

To express the selected TIL-1 gene, I designed specific primers with help of Integrated DNA Technologies server (IDT, <https://eu.idtdna.com>) that enables primer design and detection of the possible formation of hairpins, self-dimers, hetero-dimers in newly designed primers. Since I was using two approaches to ligate the TIL-1 gene into a pET-SUMO vector, I created two different pairs of TIL-1 primers (Table 2).

NEBuilder HiFi DNA Assembly mix	
FWD 5'→3'	TAAAGTACTCTAGAACTCAGGAGACAGCTCGAATTGCGGCCGACTTG
REV 5'→3'	TCCACCAATCTGTTCTCTGTG TTATGCCTTAGGCATGGGCTTGAGGG
Champion™ pET SUMO cloning kit	
FWD 5'→3'	GCAAGAATTGCGGCCGACTTG
REV 5'→3'	TCAAGCCTTAGGCATGGGC

Table 2: Primers specifically designed for TIL-1 gene used for ligation of TIL-1 with NEBuilder HiFi DNA Assembly mix (New England BioLabs) (bases highlighted in bolt represent the overhanging sequences that anneal to the linearized pET-SUMO vector) and Champion™ pET SUMO cloning kit (Thermo Fisher Scientific)

3.2.4 Cloning of TIL-1

Before cloning, the selected TIL-1 gene was amplified by PCR with Q5® High-Fidelity DNA Polymerase (New England BioLabs® Inc.). The protocol is available at the manufacturer websites (www.neb.com), and the running conditions are summarized in Table 3 below. The template was 1 µl of a cDNA pool from salivary glands of female *I. ricinus* fed for different periods to ensure most present transcripts (provided by Mgr. Kotál).

Step	Temperature [°C]	Time [s]
1	98	30
2	98	10
3	55	30
4	72	30
5	72	120
6	4	∞

Table 3: PCR profile of Q5® High-Fidelity DNA Polymerase with TIL-1 gene

As previously mentioned, ligation of the TIL-1 gene into the pET-SUMO vector was performed using two kits: NEBuilder HiFi DNA Assembly (New England BioLabs) and Champion™ pET SUMO cloning kit (Thermo Fisher Scientific).

Ligation of TIL-1 gene was performed to linearized pET-SUMO vector using NEBuilder HiFi DNA Assembly (New England BioLabs) following the manufacturer's instructions. The plasmid was transformed into TOP10 *E. coli* cells (ThermoFisher Scientific), and the cells were spread onto the preheated LB agar plates with Kanamycin (Kan, 50 µg/ml) and incubated at 37°C overnight (O/N).

To enable successful ligation of the TIL-1 gene into a pET-SUMO vector in Champion™ pET SUMO cloning kit (Thermo Fisher Scientific), I needed to create adenylated ends of the amplicon. After finishing all PCR cycles, I added Taq DNA polymerase from PCR Master Mix 5 U/µl (ThermoFisher Scientific) so that Q5 polymerase and Taq polymerase were in 1: 2.5 ratio. The PCR tubes were incubated at 72°C for 10 min. I used Champion™ pET SUMO Expression System for cloning of adenylated TIL-1 gene, where TIL-1 insert was ligated into the SUMO vector. The plasmid was transformed into One Shot® Mach1™ T1^R competent *E. coli* cells as listed in the protocol (both ThermoFisher Scientific). The cells were incubated on preheated LB agar plates with Kan at 37°C (O/N).

I performed colony PCR (protocol available online, ThermoFisher Scientific, with insert specific TIL-1 FWD primer and vector-specific SUMO-T7R primer). Tested colonies that grew on the plate were transferred onto a new LB plate. The colony PCR profile is outlined in Table 4.

Step	Temperature [°C]	Time [s]
1	95	300
2	95	60
3	46	30
4	72	60
5	72	300
6	4	∞

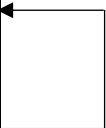


Table 4: Profile of the colony PCR

Positive colonies were grown in centrifuge flasks in LB medium with Kan. Plasmid from the miniprep was isolated with NucleoSpin Plasmid kit (Macherey Nagel). The successful transformation of selected TIL-1 insert into the plasmid and subsequent amplification in colonies was verified by sequencing the purified plasmid by SeqMe (www.seqme.eu).

3.2.5 Pilot expression of TIL-1 protein

In the pilot expression of TIL-1 inhibitor, I performed the optimization of expression and analyzed three different parameters:

- 1) expression with and without the addition of 1% glucose
- 2) expression at two different temperatures (30°C and 37°C)
- 3) expression at different time points

Prior to the pilot expression, the purified plasmid was transformed into the expression cells by adding 150 ng of the plasmid (from miniprep with confirmed sequence) to 50 µl of *E. coli* BL21 Star™ (DE3) pLysS competent cells (Invitrogen). The mixture was laid down on the ice for 20 min, followed by 1 min heat shock in 42°C water bath, and the mixture was cooled for 2 min on ice. I added 250 µl of SOC medium (Invitrogen) to the mixture and incubated at 37°C for 1 h. I mixed prepared bacterial culture with 10 ml of LB medium with Kan and incubated while shaking (150 rpm) at 37°C (O/N). 1 ml aliquots from the overnight culture were frozen in 80% glycerol at -80°C for further use, 4 ml of the O/N culture were used for the protein expression.

For the pilot expression, I mixed 50 ml of LB with Kan with 2 ml of O/N culture in cultivation flask A, and the same mixture was prepared into another flask B with the addition of 1% glucose (Sigma). Both flasks were incubated while shaking (200 rpm) till they reached OD 600 in 0.6-0.8 range (ca. 3 h). The B flask was spun down to get rid of the glucose, and I mixed the bacterial pellet with 50 ml of LB with Kan. Afterward, I added IPTG (Invitrogen) in a final concentration of 1 mM in both flasks. At this point, I split the content of both flasks A and B in half into 4 separated Erlenmeyer flasks A1, A2, B1, and B2. Flasks A1, B1 were incubated at 30°C, and A2, B2 were incubated at 37°C. I collected 1 ml of each mixture at six different time points (0, 1 h, 2 h, 5 h, 11 h, and 23 h from the expression induction). I centrifuged those aliquots down (5 min, 5 000 xg) and kept the pellet. The experiment procedure is outlined in Figure 7.

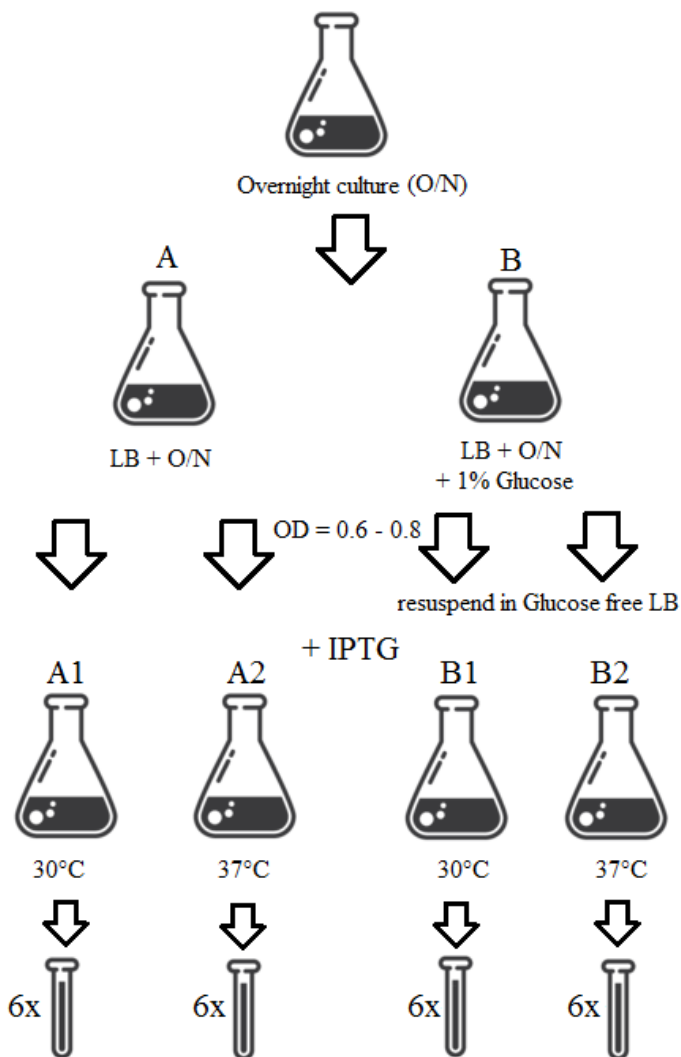


Figure 7: Scheme of pilot expression of TIL-1. The uppermost flask represents O/N culture that was split into two different flasks, A and B. 1 % of glucose was added to the B flask, and the cells were grown till optical density (OD) reached 0.6-0.8. Then, IPTG was added while incubating at 30 and 37°C (A1, A2, B1, B2), and in six different time points, 1 ml aliquots were collected and used for further analysis

To verify the presence of TIL-domain protein in bacterial cytoplasm or inclusion bodies, the cells were broken four times by freezing the supernatant in liquid nitrogen, incubating at 56°C, vortexing, and I centrifuged the supernatant for 10 min at 10 000 g. The supernatant and remaining

pellet were mixed with 7 μ l loading dye (LD), incubated at 90°C for 10 min, spun down, and analyzed by SDS PAGE.

After the optimization of protein expression, the protein was expressed on a large scale. Before the expression, I prepared 200 ml of O/N culture (1 ml glycerol stock and 200 ml of LB with Kan incubated while shaking (150 rpm) at 37°C (O/N). I split the whole volume of O/N culture into 4 liters LB with Kan into 2-liter Erlenmeyer flasks (8 flasks). The cells were incubated while shaking (200 rpm) at 37°C ca. 3 h, till OD reached a value in the range 0.6-0.8. I performed protein expression induction by adding IPTG (in final concentration 1 mM), still at 37°C while shaking (200 rpm). Cells were harvested by centrifugation (15 min, 3 000 x g, 4°C) at the optimal time point ascertained from the pilot expression. The collected pellet was frozen at -20°C.

3.2.6 Western blotting

To verify the presence of TIL-1 protein in the pellet, I dissolved a small portion of the pellet in 150 μ l of 500 mM NaCl-Tris, pH8 and I cooled the pellet in four cycles in liquid N₂, heated at 56°C in water bath and vortexed. After centrifugation (10min, 10 000xg), I mixed the supernatant (2x and 9x diluted with 500 mM NaCl-Tris) and the remaining pellet in LD, boiled at 90°C for 10 min, and performed SDS-PAGE. The gel was stained with Coomassie Brilliant Blue (CBB) for 1 h, then destained using a destaining solution for 1 h, and the remaining stain on the gel was washed in distilled water while gentle shaking (O/N). I performed Western blotting with the polyacrylamide gel according to the Electrophoretic Blotting System protocol (CBS Scientific by Fisher Scientific). After blotting the membrane, I washed it with PBS-Tween, and incubated by shaking the membrane in 3% blocking milk solution for 1 h, washed it in PBS-Tween, and incubated it with primary Anti-6xHis antibody (1:1 000 in 1% milk solution, Sigma) at 4°C (O/N). Afterward, I washed the membrane three times in PBS-Tween for 5 min and added secondary peroxidase-labeled Goat Anti Mouse antibody (1:2 000 in 1% milk solution, Sigma) at 25°C. After one hour, I washed the membrane three times in PBS-Tween, added Substrate Detection reagents (ThermoFisher Scientific), and detected the chemiluminescence signal (Uvitec, Cambridge).

3.2.7 Cell disruption

After overexpression, I needed to obtain the protein from the bacterial pellet. I did it by thawing the pellet on ice for 15 min, added 30 ml of 500 mM NaCl-Tris with Protease inhibitor cocktail (Roche). I resuspended the pellet by vigorous vortexing and added 500 mM NaCl-Tris buffer until a 50 ml volume.

The resuspended cells were disrupted three times by the French press. Afterward, I added DNase (10 mg/ml, ThermoFisher Scientific) to the resulting mixture and let it rest on ice for 20 min. Ultracentrifugation of the disrupted cells was the next step. The supernatant was frozen at -80°C.

3.2.8 Protein purification

The supernatant containing TIL-1 protein was purified by Nickel-affinity chromatography using HisTrap FF 5ml column (GE Healthcare). In further experiments, I needed to cleave the His-SUMO tag from the TIL-1 protein. For this purpose, His-SUMO tagged TIL-1 was resuspended in 20 mM Tris to dilute the NaCl concentration in the sample (NaCl inhibits the SUMO-protease). I mixed 15 ml of 20 mM Tris solution containing TIL-1 with 1 mM DTT and incubated with 15 µl of SUMO protease (Invitrogen) while gentle shaking at 25°C O/N.

In order to figure out as most precise concentration of purified TIL-1 protein possible, I used Bradford Albumin calibration curve from Pierce BCA protein assay kit (ThermoFisher Scientific), where bovine serum albumin (BSA, Sigma) was used to generate a standard curve.

3.2.9 Coagulation assays

In the scope of this thesis, I performed three coagulation assays: Activated Partial Thromboplastin Time (aPTT), Prothrombin Time (PT), and Thrombin Time (TT). Each coagulation assay was done in a coagulometer (Ceveron® four, Technoclone) at 37 °C. In case TIL-1 protein showed inhibition of coagulation at the highest selected concentration of 6 µM, I lowered the concentration of TIL-1 stepwise to verify the lowest inhibitory concentration of the TIL-1 inhibitor. Coagulation was done in triplications (with TIL-1, SUMO tag as the inhibitory specificity control, and PBS as the coagulation control) in each assay. The exact procedures of each assay are described below.

3.2.9.1 aPTT

In aPTT assay (Hemker et al., 1986), 100 μ l of plasma (Coagulation Control N) and 6 μ M TIL-1 inhibitor were incubated in coagulometer for 10 min. At the same time, I incubated plasma with PBS instead of TIL-1 inhibitor (in the same concentration). Afterward, I added to each well 100 μ l of Dapptin reagent and incubated the mixtures for another 2 min. The addition of CaCl₂ solution triggered coagulation.

3.2.9.1 PT

In PT assay (Langdell et al., 1953), 100 μ l of plasma and 6 μ M TIL-1 inhibitor were incubated in coagulometer wells for 10 min. At the same time, I incubated plasma with PBS instead of TIL-1 inhibitor (in the same concentration). The addition of Technoplastin reagent triggered coagulation.

3.2.9.2 TT

In TT, 200 μ l of plasma and 6 μ M TIL-1 protein were incubated in coagulometer for 10 min. At the same time, I incubated plasma with PBS instead of TIL-1 inhibitor (in the same concentration). The addition of 200 μ l of Thrombin reagent started the coagulation of plasma.

3.2.10 Thrombin assay

To check whether TIL-1 protein from *I. ricinus* inhibits thrombin activity, a thrombin assay was performed. I wanted to define whether the TIL-1 inhibitor inhibits thrombin proteolytic activity by competing with the fluorescently labeled substrate in the thrombin assay. I incubated 100 μ l of reaction mixture composed of 40 pM Thrombin (Sigma), 5 μ M TIL-1 protein diluted in thrombin assay buffer at RT in a non-transparent 96-well plate. After 10 min of incubation, I added fluorescent substrate (Boc-Val-Pro-Arg-7-amido-4-methylcoumarin hydrochloride (Boc-VPR-AMC, Sigma) to the final concentration 250 μ M and inserted the plate into the Synergy H1 microplate reader (BioTek, Winooski, USA) where it was shaken for 15 s at 37 °C. Afterward, I measured the fluorescence (excitation at 365 nm, emission at 450 nm) and the data were collected for 20 min in 1 min intervals.

The evaluation of the data obtained from the thrombin assay was done in Microsoft Office Excel. During the thrombin assay, the fluorescence intensities of a control reaction mixture (without

inhibitors), reaction mixture with TIL-1 protein, and SUMO tag were recorded by the microplate reader. The fluorescence intensity time points were used to create a linear regression. The regression line slope was calculated in percent and used as the relative fluorescence units (RFU).

3.2.11 Trypsin assay

Trypsin assay was performed to verify the expected inhibition of trypsin by TIL-1 inhibitor. In this assay, I incubated 50 μ l of a reaction mixture prepared from 20 pM Trypsin from bovine pancreas (Sigma) with trypsin assay buffer at RT in a non-transparent 96-well plate. After 10 min, I added 250 μ M fluorescent substrate (Boc-VPR-AMC, Sigma) and inserted the plate into the Synergy H1 microplate reader (BioTek, Winooski, USA), where it was shaken for 15 s at 37 °C. Afterward, the fluorescence was measured (excitation at 365 nm, emission at 450 nm), and the data were collected for 20 min in 1 min intervals.

The evaluation of the trypsin assay data was done the same way as in the thrombin assay.

3.2.12 LPS decontamination

Since the isolated TIL-domain protein was expressed in *E. coli*, the sample contained large amounts of lipopolysaccharide (LPS) from the *E. coli* cell walls. Via Toll-like receptors (TLR), LPS strongly activates innate immunity (Doerrler, 2006). With the help of the lipid-A chain, it stimulates monocytes, neutrophils, and macrophages. It activates the complement and coagulation system, and the leukocytes migrate towards LPS due to chemotaxis (Liu et al., 2019). Therefore, prior to the immunologic assays, the sample containing TIL-1 protein was purified from the excessing LPS with ToxinEraser Endotoxin Removal Kit (GenScript). The samples were measured for the presence of remaining LPS with PyroGene Recombinant Factor C Endotoxin Detection Assay (Lonza) using Synergy H1 microplate reader (BioTek, Winooski, USA).

3.2.13 Immunologic assays

3.2.13.1 Isolation of monocytes

Leukocytes were isolated from the bone marrow of murine femur and tibia (mouse C57bl6, 10 weeks old). The bones' endings were cut, and the bone marrow was washed out with 26G needle attached to a syringe with 50 ml RMPI medium. The suspension was filtered through 70 μ m nylon

cell strainer (Corning) into 50 ml centrifuge tubes. I centrifuged the cells in centrifuge with a swing-out rotor at 250 g, for 5 min at 4°C. I aspirated the supernatant and resuspended the pellet in 5 ml of RPMI medium. To remove erythrocytes, I added 1 ml of Red-Blood-Cell Lysis Buffer (eBioscience) and incubated 2 min at 25°C. By adding PBS till 15 ml, the lysis of other cells was stopped, and I centrifuged the solution (swing-out rotor, 250 g, 5 min, 4°C). I aspirated the supernatant and washed the pellet two more times with PBS.

To isolate monocytes from the murine bone marrow cells, I used Monocyte Isolation Kit (BM) mouse (MACS, Miltenyi Biotec) following the manufacturer's instructions (www.miltenyibiotec.com). The isolation was performed using magnetic separation with MACS LS Column (MACS, Miltenyi Biotec).

3.2.13.2 Monocyte adhesion

I coated the costar 3590-96 well EIA/RIA Plate with 50 µl of 10 µg/ml proteins of extracellular matrix (laminin, fibronectin, and collagen, all purchased by Sigma) 24 h before the monocyte adhesion assay.

The isolated monocytes were stained using 5 µM Cell Proliferation Dye eFluor™ 670 (eBioscience) at 37°C for 10 min. The cells were washed 3 times with 15 ml of PBS from the excessing dye (swing-out rotor, 250 g, 5 min, 4°C).

I counted the monocytes by staining 10 µl of cells in monocyte isolation buffer with 90 µl of 0.2% trypan blue solution (Sigma) using a hemocytometer under the optical microscope.

Afterward, I split the cells into four 1.5 ml Eppendorf tubes and incubated 250 µl of the stained monocytes with 4 µM and 2 µM TIL-1 inhibitor, 4 M pET-SUMO tag (both LPS-free) at 37°C for 2 h. One portion of stained monocytes was incubated without any inhibitor as control.

I removed the unbound proteins of the extracellular matrix from the 96-well plate and blocked the plate with 100 µl of 3 % BSA (fatty acid-free) one hour before the actual adhesion experiment. The remaining BSA was removed from the wells after blocking.

The monocytes were activated by adding 200 ng/ml PMA (phorbol 12-myristate 13-acetate, Sigma) and pre-incubated at 37°C for 20 min. The four mixtures were diluted with 1 ml of RPMI

medium (BioSera). I divided 100 μ l of the monocyte mixture onto the protein-coated wells on the plate (20 000 cells into one well). Simultaneously, I split 100 μ l of the monocyte mixture onto 3 % BSA blocked wells (without extracellular matrix proteins) to show that the monocytes do not adhere to the BSA molecules. The plate was incubated at 37°C for 1 h. The fluorescence representing added cells was measured at excitation 640 nm and emission 670 nm using Synergy H1 microplate reader (BioTek, Winooski, USA). Then, the plate was washed with 100 μ l of PBS, and the fluorescence was measured again. I repeated this process four times.

The adhered cells were counted as a percentage from the difference between the first and the second washing step of the plate. Afterward, I calculated the means from the triplicates and the standard deviation of the mean. The statistical significance of the results was proved by Student's *t*-test in Microsoft Office Excel.

3.2.14 Expression profile of TIL-1

In order to reveal the expression profile of the TIL-1 inhibitor, I performed quantitative PCR (qPCR) on C1000 Touch™ Thermal cycler. As the templates, I chose cDNA from salivary glands, midgut, and ovaries from adult *I. ricinus*. For this purpose, I designed another pair of primers suitable for qPCR run, as shown in Table 5 below.

TIL-1	
FWD 5' → 3'	CAAGAATTGCGGCCGACTTG
REV 5' → 3'	CCCTTACGGTAGAAGCCTGG
EF-1	
FWD 5' → 3'	CTGGGTGTGAAGCAGATGAT
REV 5' → 3'	GTAGGCAGACACTTCCTTCTG

Table 5: Primers for TIL-1 gene and elongation factor 1 (EF-1) used in qPCR

The reaction mixture was composed of 5 μ l of Master Mix FastStart Universal SYBR® Green Master (ROX) (Roche), 3.4 μ l of ultrapure water, and 0.3 μ l of each FWD and REV primers (both 10x diluted), all per 1 reaction. I pipetted the master mix precisely into qPCR tubes and added 1 μ l of 5x diluted cDNA. I gently vortexed and spun the tubes down.

To enable comparison of values from different samples, they were normalized against a reference gene elongation factor 1 (EF-1). Hence, the same reaction mixture was prepared, only instead of specific TIL-1 primers, elongation factor primers (EF-1 FWD and REV) were added in the same amount.

The profile of the qPCR run is summarized in Table 6.

Step	Temperature [°C]	Time [s]
1	95	180
2	95	10
3	60	30
4	60	31
5	4	∞

Table 6: qPCR profile with the analysis of melting curve at steps 5-6

In the evaluation of the expression profile of TIL-1, I calculated a relative ratio of TIL-1 molecules by using following formula:

$$\text{Relative ratio of TIL-1} = \text{efficacy of primers}^{\wedge} \text{Cq (EF-1)} / \text{efficacy of primers}^{\wedge} \text{Cq (TIL-1)},$$

where the efficacy of primers equals 2 (means that two strands of cDNA replicates are created by one primer pain in one qPCR cycle), Cq (Quantification cycle) refers to the values obtained from C1000 Touch™ Thermal cycler software (BioRad), and EF-1 means the reference gene elongation factor 1 used for normalization.

Afterward, I normalized the relative ratios to the highest value of TIL-1 and assumed this value as a 100 % expression. I divided the remaining relative ratios of TIL-1 molecules by the highest expression value, multiplied by 100, and obtained the percentage of relative expression of TIL-1 protein in each tissue.

4 Results

4.1 Bioinformatics of TIL-domain inhibitors of *I. ricinus*

Based on the alignment done by ClustalW Multiple alignment in BioEdit, the sequences were arranged according to the conserved core composed of 10 cysteines. The cysteine residues were either ordered in groups (designated as C1-C10, as shown in Figure 8), or they were slightly shifted based on different insertions or deletions in individual sequences.

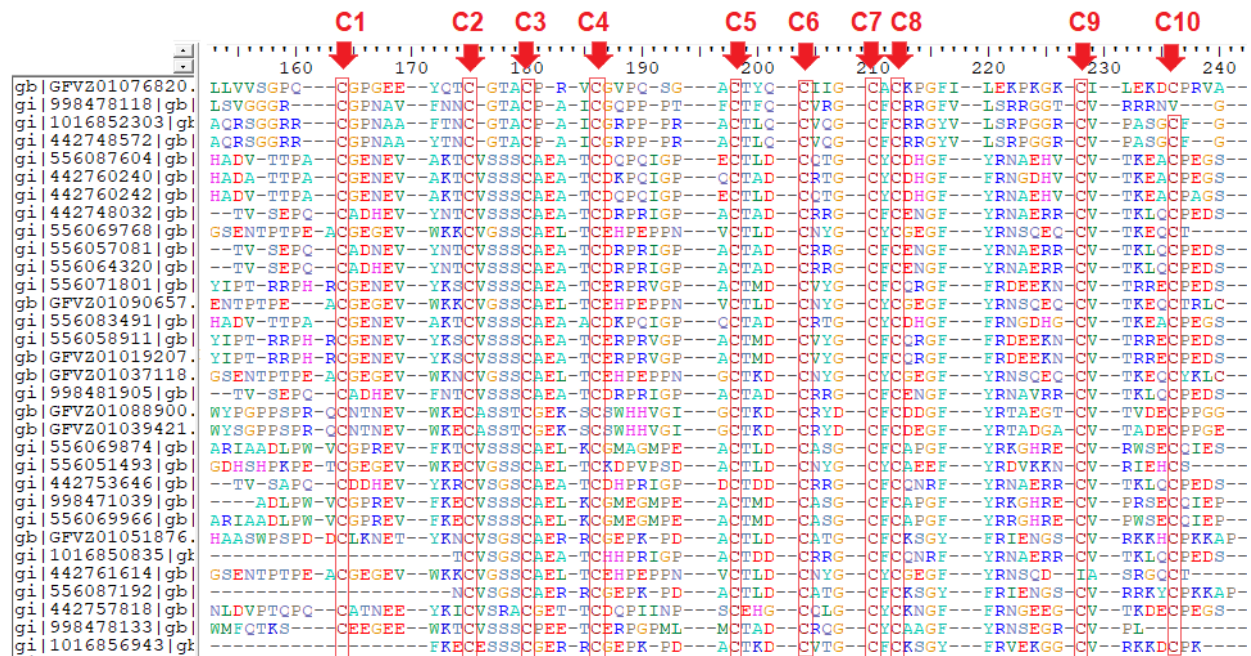


Figure 8: Part of an alignment of TIL-domain proteins from *I. ricinus* containing conserved cysteine core. Later in phylogenetic analysis, the first four sequences were clustered together, and this way, I selected TIL-1 protein representative

Based on the phylogeny, I classified the TIL-domain proteins from *I. ricinus* into 17 groups (Figure S1 in Supplement). There I marked each group as TIL-1 till TIL-17, and for each group, I chose one representative protein with the most similar sequence to the others from one group (Figure 9).

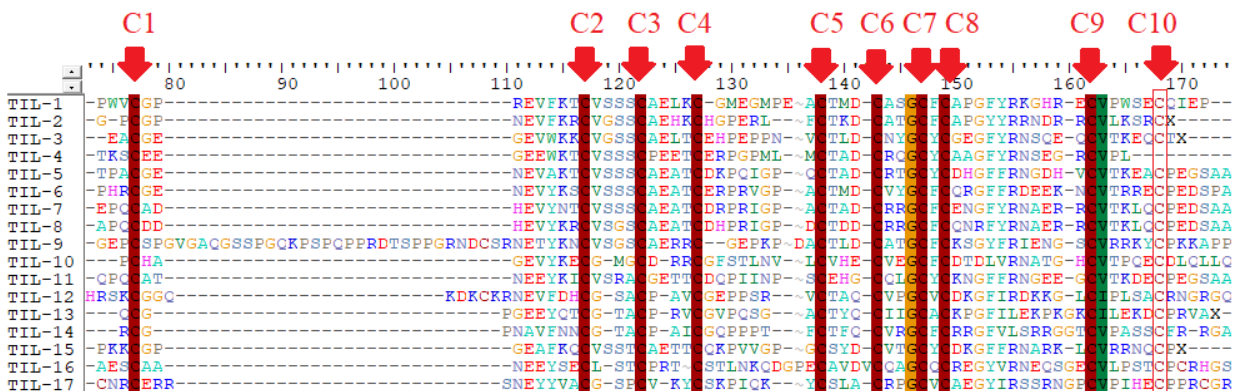


Figure 9: ClustalW alignment of selected 17 representatives of TIL-domain inhibitors of *I. ricinus*. The 10 conserved cysteine residues are indicated with arrows

Selected 17 TIL-domain inhibitors were aimed to be analyzed by creating recombinant proteins. In the scope of this thesis, I focused on the analysis of only one TIL-domain inhibitor: TIL-1 (results summarized below).

According to the BLAST search, the TIL-1 protein belongs to the protein family pfam 01826; “Trypsin inhibitor like cysteine-rich domain” (TIL).

4.2 Protein structure prediction

Using Swiss Model and LOMETS I obtained multiple possibilities of TIL-1 protein structure prediction, as shown below.

4.2.1 Swiss Model output

According to the Swiss Model results, the most reliable structure prediction was according to chymotrypsin inhibitor of *A. mellifera* chymotrypsin inhibitor (AMCI, PDB: 1ccv) with GMQE 0.45 and QMEAN -1.53 (Figure 10).

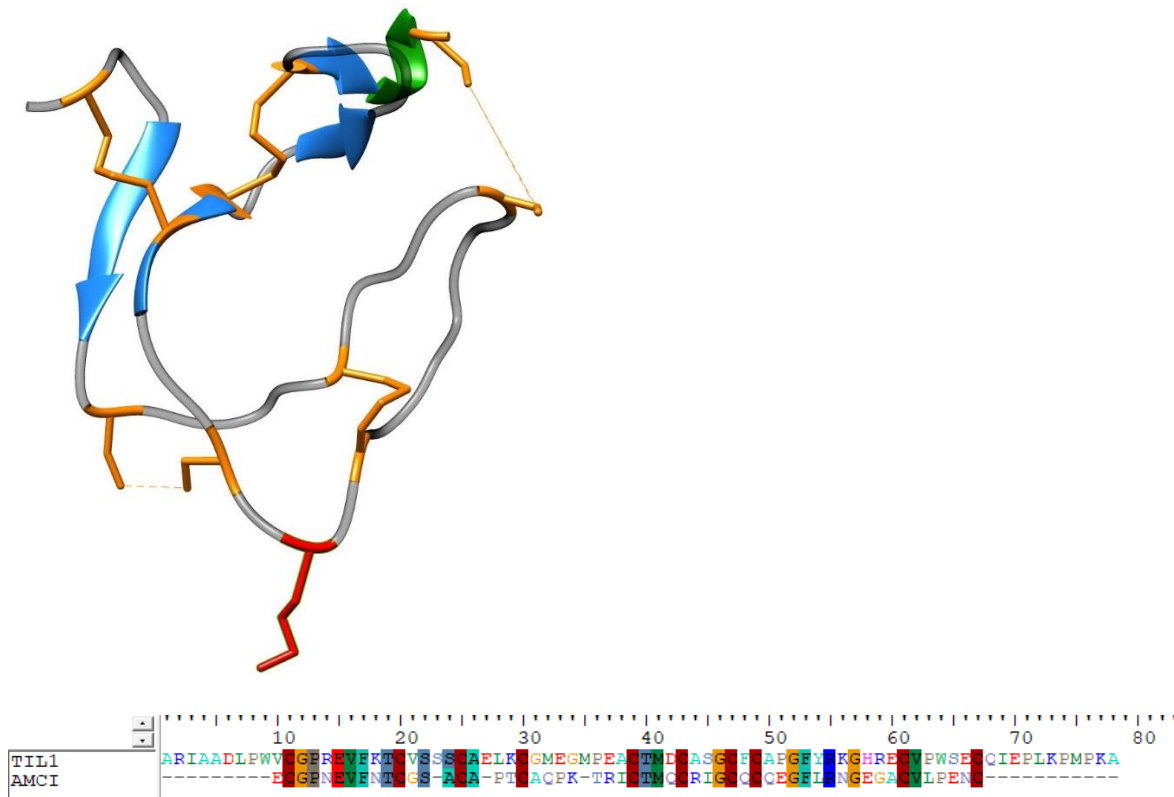


Figure 10: TIL-1 protein structure prediction according to *A. mellifera* chymotrypsin inhibitor AMCI (PDB: 1ccv). One short α -helix is colored in green, 4 short β -sheets in blue, the coil in grey, 10 cysteines with 5 incompletely created disulfide bridges in orange, the red active site P1 is expected at Met41 (similar to AMCI with P1 at Met30) (edited in UCSF Chimera). The lower picture shows the sequence alignment of target TIL-1 and AMCI with highlighted conserved regions (created in BioEdit)

Another promising model was built according to a complex of *Ascaris* chymotrypsin/elastase inhibitor with porcine elastase (PDB: 1eai) with GMQE 0.36 and QMEAN: -2.64 (Figure 11).

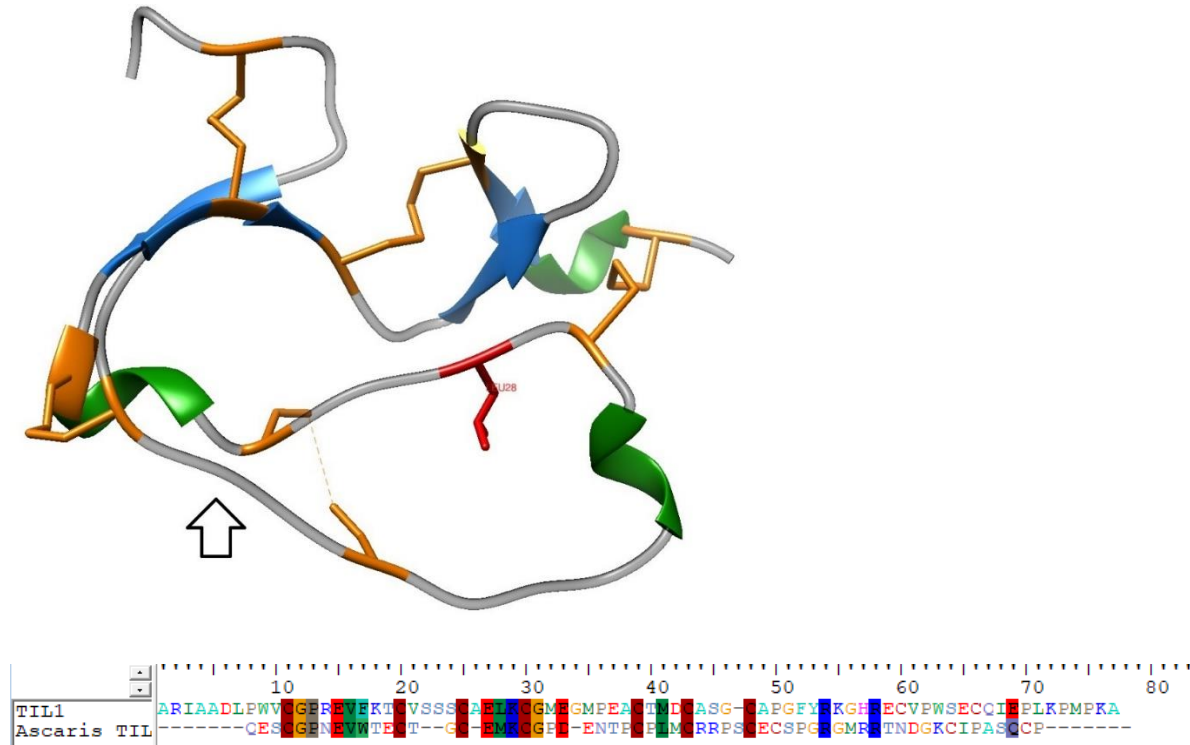


Figure 11: TIL-1 protein structure prediction according to *Ascaris* chymotrypsin/elastase inhibitor complex (PDB: 1eai). Three short α -helices are colored in green, 4 short β -sheets in blue, the coil in grey, 10 cysteines with 5 disulfide bridges in orange, the red active site P1 should resemble at Leu28 (similar to *Ascaris* chymotrypsin/elastase inhibitor with P1 at Leu31) (edited in UCSF Chimera). The arrow indicates the expected position of the P1 site at Met41 (between 5th and 6th cysteine residues). The lower picture shows the sequence alignment of target TIL-1 and *Ascaris* chymotrypsin/elastase inhibitor (marked as Ascaris TIL) with highlighted conserved regions (created in BioEdit)

Other model showed some reliable results too (see the structure in Figure 12). That was built based on the structure of BSTI, a trypsin inhibitor from *B. bombina* (PDB:1hx2). Although, the reliability of quality estimation was slightly lower (GMQE: 0.32 and QMEAN: -2.24).

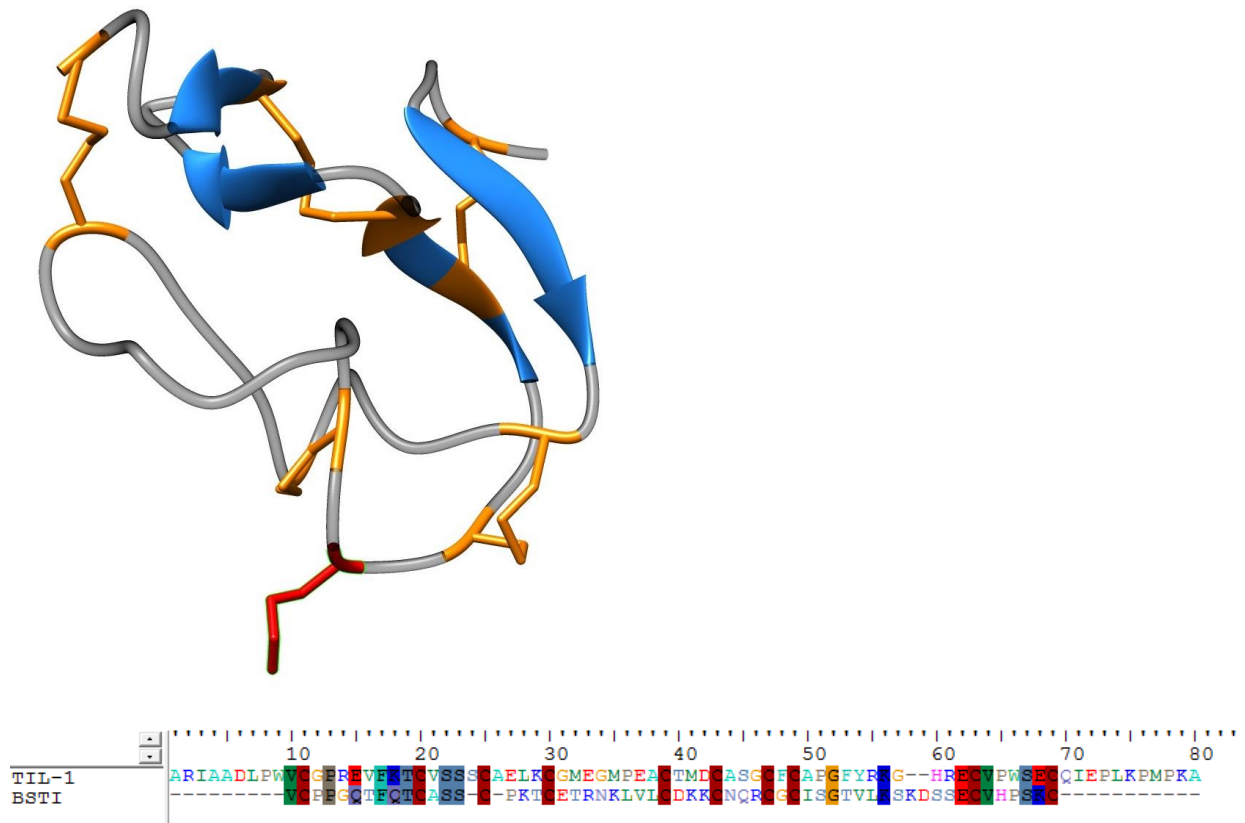


Figure 12: TIL-1 protein structure prediction according to BSTI from *B. bombina* (PDB:1hx2). 4 short β -sheets in blue, the coil in grey, 10 cysteines with 5 disulfide bridges in orange, the red active site P1 is expected at Met41 (in comparison to *B. bombina* with P1 at Glu32) (edited in UCSF Chimera). The lower picture shows the sequence alignment of target TIL-1 and BSTI from *B. bombina* (marked as BSTI) with highlighted conserved regions (created in BioEdit)

4.2.2 LOMETS

From the LOMETS server, I obtained 3 top templates with a normalized Z-score ≥ 1 , which is supposed as a good alignment (Wu and Zhang, 2007, Zheng et al., 2019). Protein model with the highest normalized Z-scores (3.66, 3.13, and 3.08) was according to the structure of BSTI, a trypsin inhibitor from *B. bombina* (PDB: 1hx2), AMCI chymotrypsin inhibitor from *A. mellifera* (PDB: 1ccv) and *Ascaris* chymotrypsin/elastase inhibitor complex (Ascaris-TIL) (PDB: 1eai). The three models are depicted in Figure 13 below.

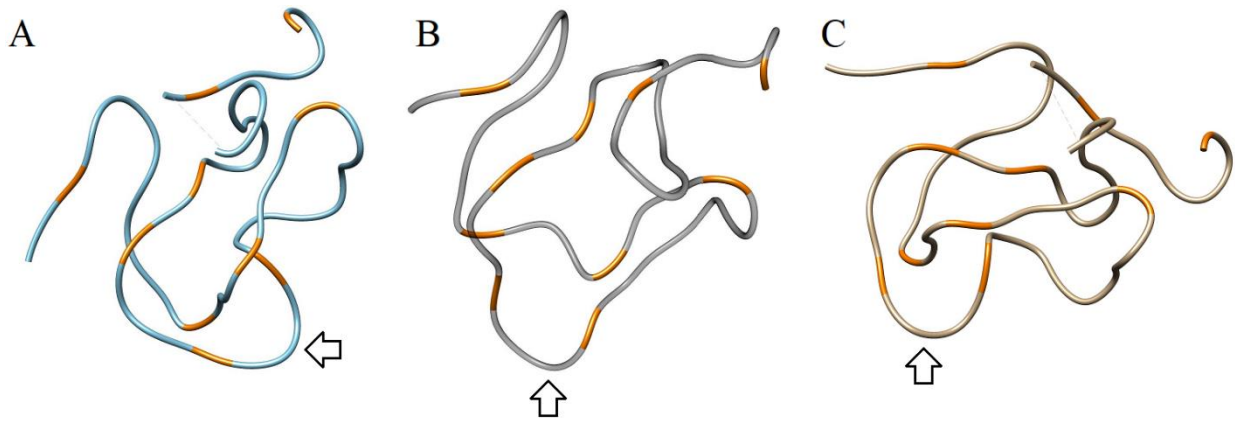


Figure 13: TIL-1 protein structure predictions according to A) BSTI (PDB: 1hx2) B) AMCI (PDB: 1ccv) and Ascaris-TIL (PDB: 1eai). The inhibitory loops are indicated with the arrows (A) BSTI model of TIL-1 at Lys32, B) AMCI model of TIL-1 at Met30, and C) Ascaris-TIL model of TIL-1 at Lys32)

Similarly, LOMETS indicated my target protein that it possibly provides with serine-type endopeptidase inhibitor activity.

LOMETS does not provide the model structures with α -helices or β -sheets. Moreover, all three model structures of TIL-1 proteins exposed binding loops in different positions (as described later in Discussion).

4.2.3 Comparison of predicted structures

I compared the resulting predicted structures obtained from Swiss model and LOMETS to see some similarities in the structures and amino acids at each P1 site (Figure 14).

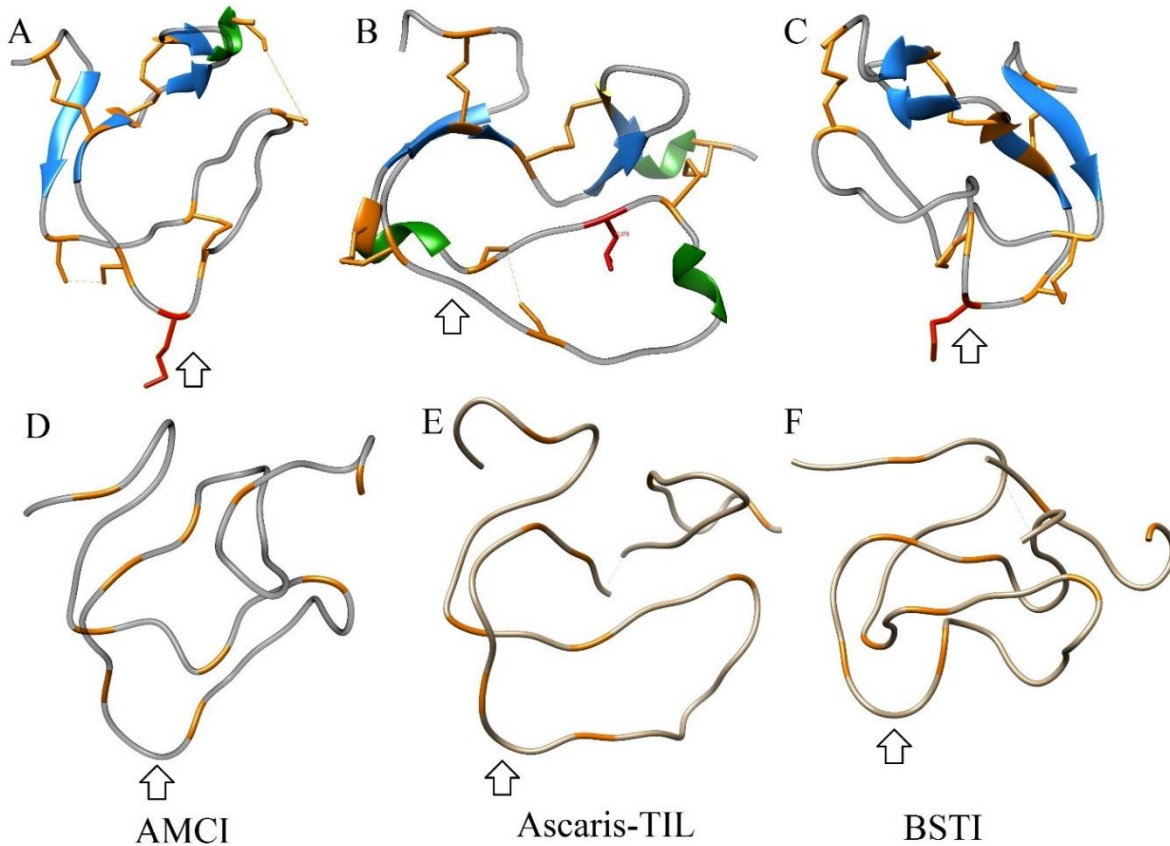


Figure 14: Comparison of model structures of TIL-1 protein. The model structures were built in Swiss model according to A) *A. mellifera* AMCI inhibitor (P1 at Met41), B) *Ascaris* chymotrypsin/elastase inhibitor complex (marked as Ascaris-TIL)(P1 at Leu28) and C) BSTI trypsin inhibitor from *B. bombina* (P1 at Met41). The model structures built by LOMETS are indicated as follows: D) *A. mellifera* AMCI inhibitor (P1 at Met30), B) Ascaris-TIL (P1 at Lys32), and C) BSTI trypsin inhibitor from *B. bombina* (P1 at Lys32). The arrows indicate the expected P1 site of each model TIL-1 protein

According to Figure 14, the amino acid at P1 sites of each TIL-1 model differ. The varying P1 sites in reference to TIL-domain structures and the P1 sites of model structures are summarized in Table 7 below.

	Original P1	Swiss model	LOMETS
AMCI	Met30	Met41	Met30
Ascaris-TIL	Leu31	Met41	Lys32
BSTI	Glu32	Met41	Lys32

Table 7: The active sites of TIL-domain inhibitors (Original P1) and predicted *I. ricinus* TIL-1 protein structures by Swiss model and LOMETS protein structure prediction servers. AMCI- cathepsin G/chymotrypsin inhibitor from *Apis mellifera*, Ascaris-TIL- *Ascaris* chymotrypsin/elastase inhibitor complex, BSTI- trypsin inhibitor from *B. bombina*

The most conserved position of the P1 active site in template TIL-domain proteins and the predicted TIL-1 structures is in AMCI inhibitor. According to the AMCI inhibitor, the P1 position is predicted at methionine residues, as shown from two independent protein structure modeling results.

4.3 Preparation of TIL-1 protein

The gene-specific TIL-1 primers annealed to the TIL-1 cDNA and TIL-1 transcript was amplified using Q5® High-Fidelity DNA Polymerase, as proved by agarose gel (1%) electrophoresis, as shown in Figure 15.

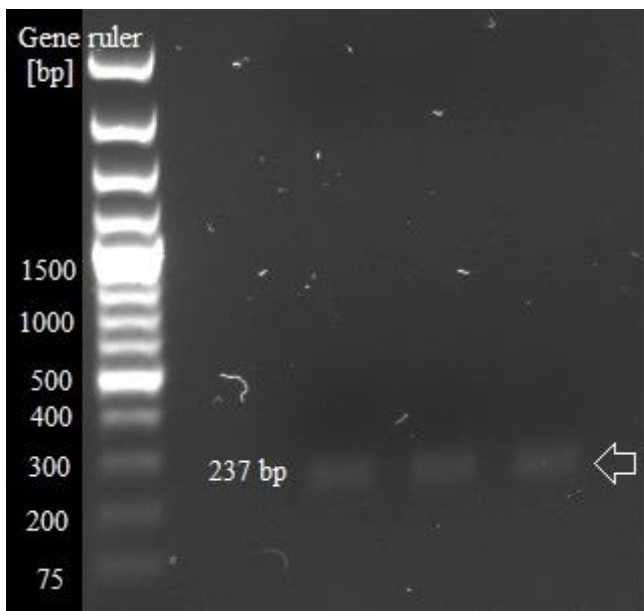


Figure 15: Agarose gel (1%) with TIL-1. The arrow is pointed to 237 bp containing the TIL-1 amplicon. I used Thermo Scientific™ GeneRuler 1 kb Plus DNA as a ladder

4.3.1 Transformation of a plasmid into *E. coli*

Ligation of TIL-1 gene was performed multiple times to linearized pET-SUMO vector using NEBuilder HiFi DNA Assembly (New England BioLabs) followed by the plasmid transformation into TOP10 *E. coli* cells (ThermoFisher Scientific). During the repeated ligations and transformations, I was optimizing several conditions. The colony PCR was, nevertheless, always negative.

The alternative and successful strategy was ligation of TIL-1 using the Champion™ pET SUMO cloning kit (Thermo Fisher Scientific). The plasmid was transformed into One Shot® Mach1™ T1^R competent *E. coli* cells, and the transformation was confirmed by colony PCR. The colony PCR result was visualized by SDS-PAGE (Figure 16).

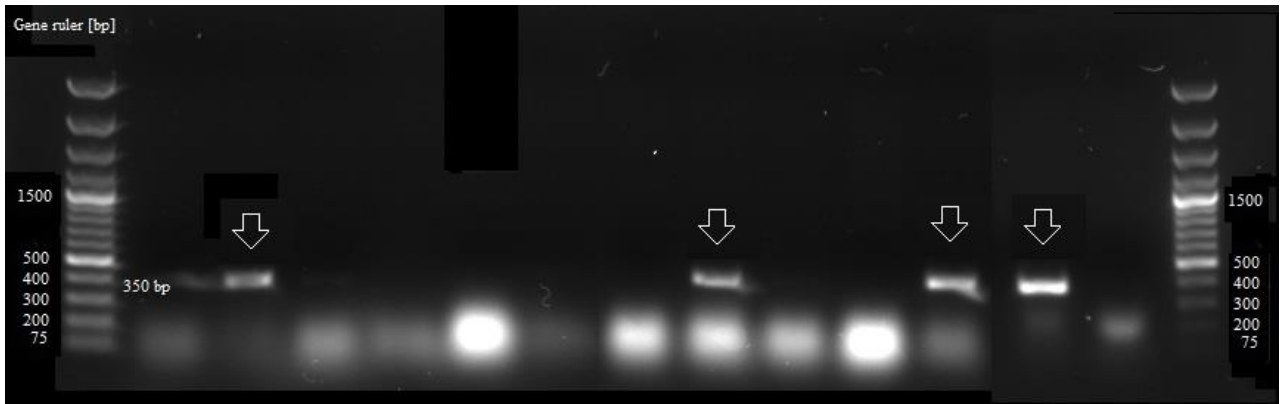


Figure 16: Colony PCR as proof of successful cloning and plasmid transformation on agarose gel (1%). The arrows in the gel indicate bacterial colonies containing TIL-1 gene transferred into pET SUMO vector with the expected size of 350 bp

4.3.2 Pilot expression of TIL-1 protein

After the colony PCR, the TIL-1 gene in Champion™ pET SUMO plasmid was isolated from One Shot® Mach1™ T1R and transformed for protein expression into BL21 Star™ (DE3) pLysS *E. coli* cells (Invitrogen). The result of pilot expression with 3 different conditions is shown in Figure 17.

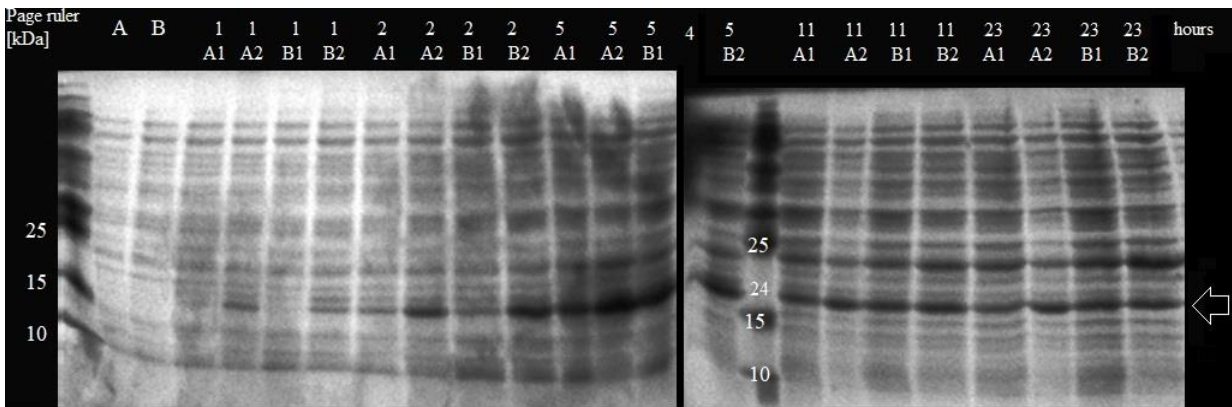


Figure 17: Pilot expression of TIL-1 protein. The arrow indicates the expected size of ca. 24 kDa of expressed TIL-1 (9.9 kDa) with His-pET-SUMO vector (14.1 kDa). Single wells are labeled with hours of incubation after induction of expression with IPTG (time points 0- 23 h). A and B wells represent incubation without and with the presence of 1 % glucose, respectively. After

adding IPTG, the expression was incubated at 30°C (A1, B1) and 37°C (A2, B2) as outlined in the pilot expression scheme in chapter Methods)

From the pilot expression, I deduced that for large scale protein expression, the addition of 1% glucose prior to IPTG induction had no positive effect on expression (B samples), 37°C seemed as optimal temperature for expression (A2 samples), and expression longer than 5 h did not increase the amount of expressed protein.

Therefore, large-scale expression of TIL-1 protein was performed without the addition of glucose. Following IPTG induction, the bacteria were incubated for 3 hours at 37°C.

4.3.3 Western blotting

After TIL-1 protein overexpression, the bacterial cells were harvested by ultracentrifugation. I checked the presence of TIL-1 protein in the supernatant (SNT) of bacterial cytosol and in the bacterial pellet performing SDS-PAGE and Western blotting. Both supernatant and the pellet contained high concentrations of the protein of interest. Using Anti-His primary antibody, the pET-SUMO (containing His-tag) + TIL-1 protein complex was visualized by Western blot as shown in Figure 18 below.

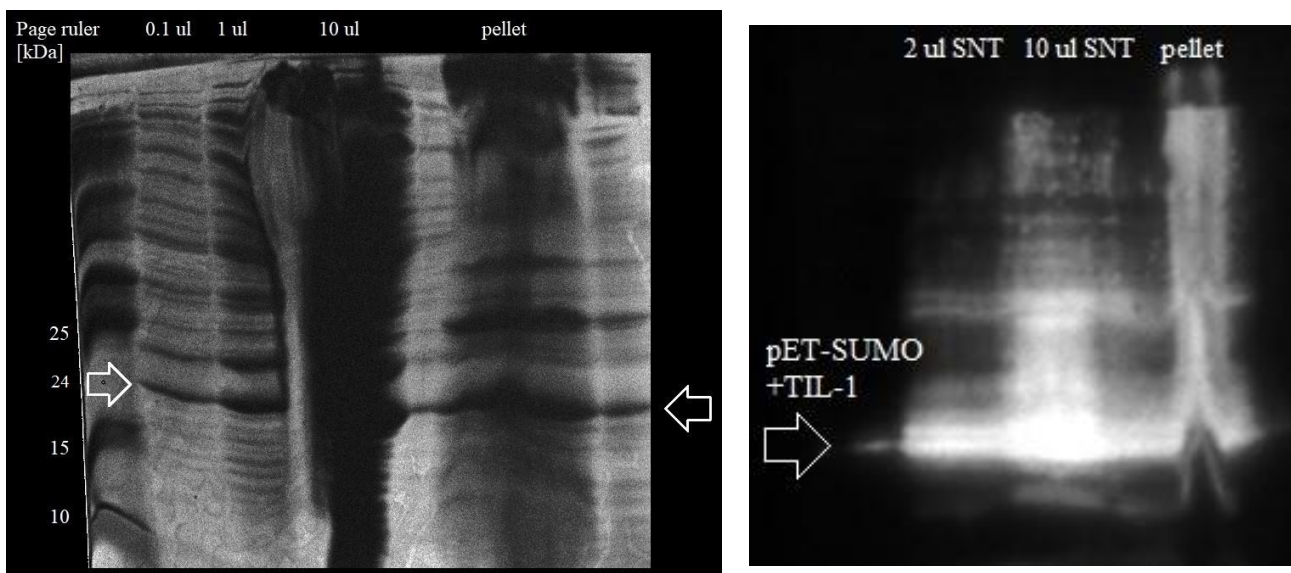


Figure 18: SDS-PAGE with pET-SUMO +TIL-1 at ca. 24 kDa (left) and Western blotting of the same polyacrylamide gel (right)

The pellet was resuspended in Tris-NaCl buffer, and the cells were mechanically disrupted by the French press.

4.3.4 Affinity chromatography

After ultracentrifugation, the supernatant was purified by affinity chromatography.

The TIL-1 protein was in the form of SUMO fusion protein, as shown in Figure 19.

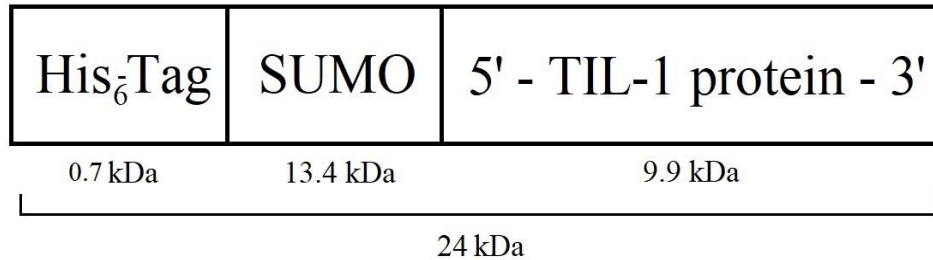


Figure 19: Scheme of the TIL-1 tagged protein with polyhistidine (His₆-tag) and SUMO tag with molecular weight ca. 24 kDa

Already after first nickel affinity chromatography, the TIL-1 tag-protein complex seemed significantly purer (Figure 20). To enable the cleavage of the tertiary structure of the ubiquitin-like protein of SUMO-tag, a high concentration of imidazole in buffer was removed by spinning the sample on Amicon® Ultra-2 Centrifugal Filters with 3 kDa molecular weight cut-off. The collected tag-protein complex was washed 3 times with cleavage buffer (20 mM Tris, 150 mM NaCl, 1 mM DTT, pH 8) on the same Amicon, and I added the cleavage buffer up to 15 ml. I added SUMO protease (Invitrogen) at 1 μM final concentration and incubated the reaction mixture at 25°C while slow shaking O/N. The result of the cleavage reaction was analyzed by SDS-PAGE (12%) the other day (Figure 20).

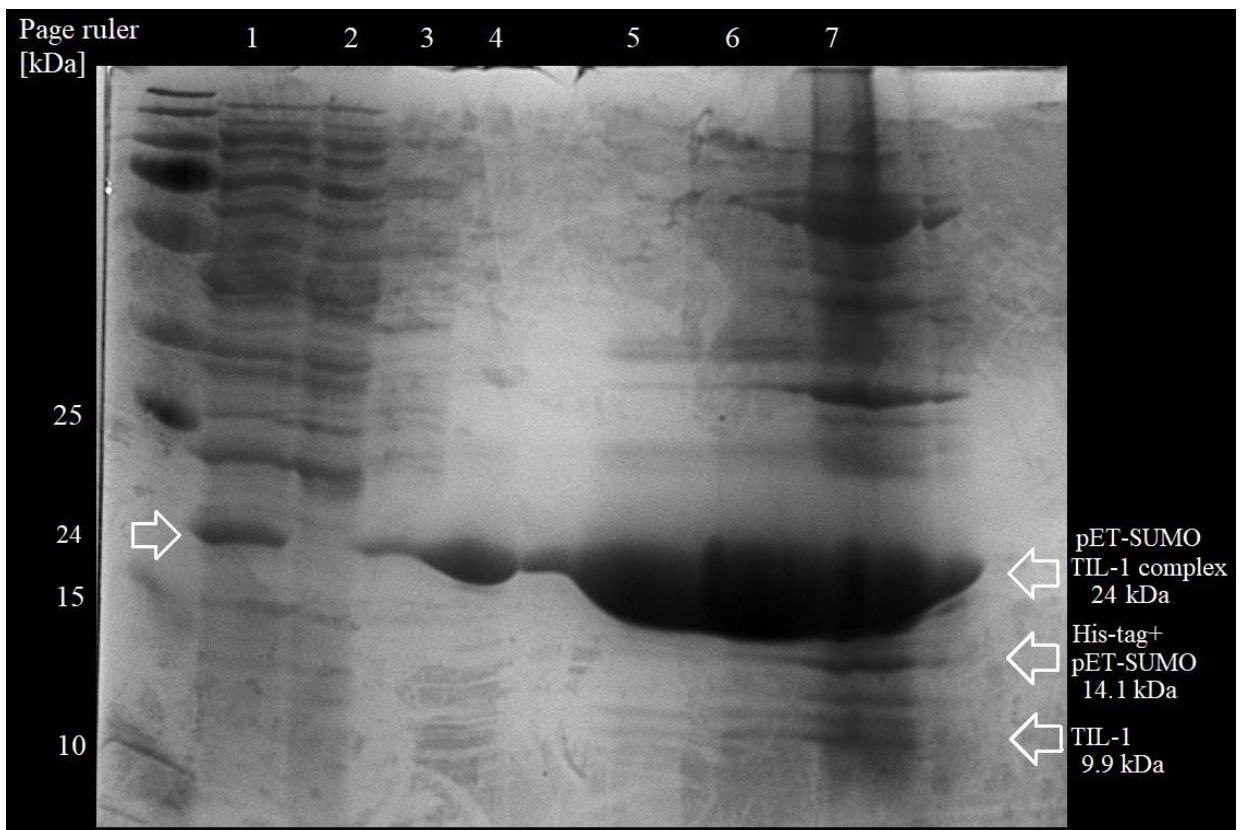


Figure 20: Affinity chromatography of TIL-1. 1) Sample after French press, the arrow indicates the band of interest (pEt-SUMO + TIL-1 complex, ca. 24 kDa); 2) flowthrough after first nickel affinity chromatography where the tag-protein complex was captured on column (the band is missing); 3) the column was washed with 20 mM imidazole, that caused weak elution of the tag-protein complex; 4) the column was washed with 200 mM imidazole which caused complete elution of the tag-protein complex; 5) 1 μ l of SNT after pET-SUMO cleavage with SUMO protease (Invitrogen); 6) 2 μ l of the same content as in 5); 7) precipitate after SUMO protease (Invitrogen) cleavage, the arrows indicate complex or cleaved complex components in the precipitate.

Since the majority of the TIL-1 protein remained attached to the His-SUMO tag, I tried to optimize the cleavage conditions. I used two kinds of SUMO-proteases: SUMO-protease from Invitrogen and ULP1 protease provided by Macrocomplex group, at the Faculty of Science, University of South Bohemia. The cleavage reaction was performed at 4°C and 25°C, O/N.

The His-SUMO tag cleavage attempts were analyzed by polyacrylamide gels (12%), depicted in Figure 21.

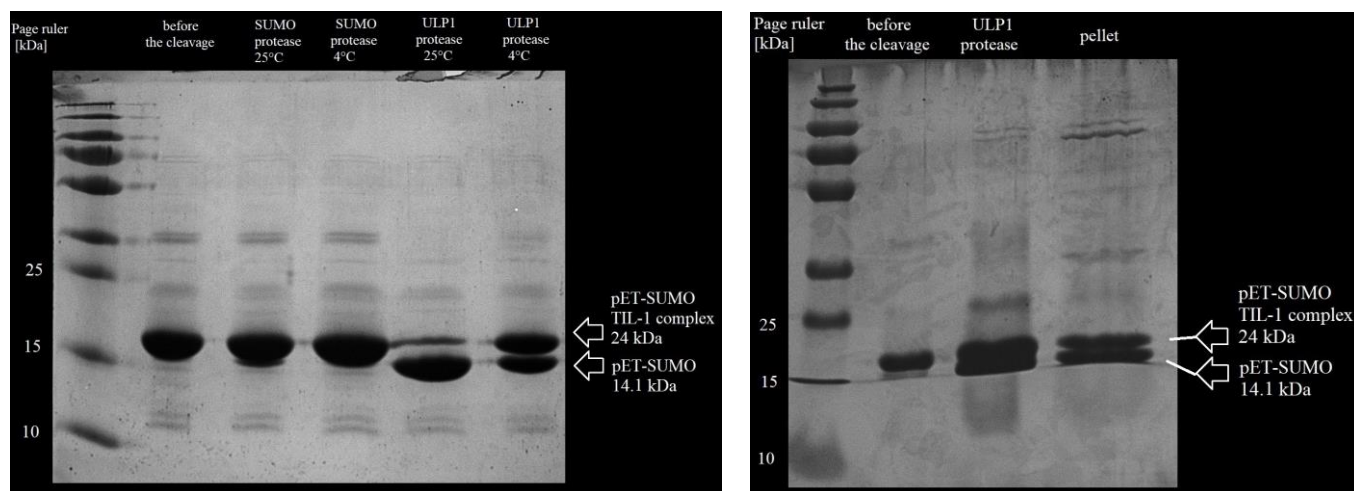


Figure 21: Cleaving of His-pET-SUMO tag attached to TIL-1 protein. SUMO-protease (Invitrogen) and ULP1 protease (Macrocomplex group, FS, USB) cleavage at 25°C and 4°C, O/N (left); Efficient cleavage of ULP1 protease performed at 25°C, O/N, with a precipitate that formed a pellet in the vial

To stabilize the target protein in the cleavage reaction, I added 60 mM L-Arginine (ThermoFisher Scientific).

Since the His-SUMO tag seemed to be cleft from the tag-protein complex and none of the gels visualized a clear band representing TIL-1 protein, I performed second affinity chromatography to trap the cleaved tag and to collect the desired TIL-1 protein in flow through. The result of the second affinity chromatography is shown in Figure 22.

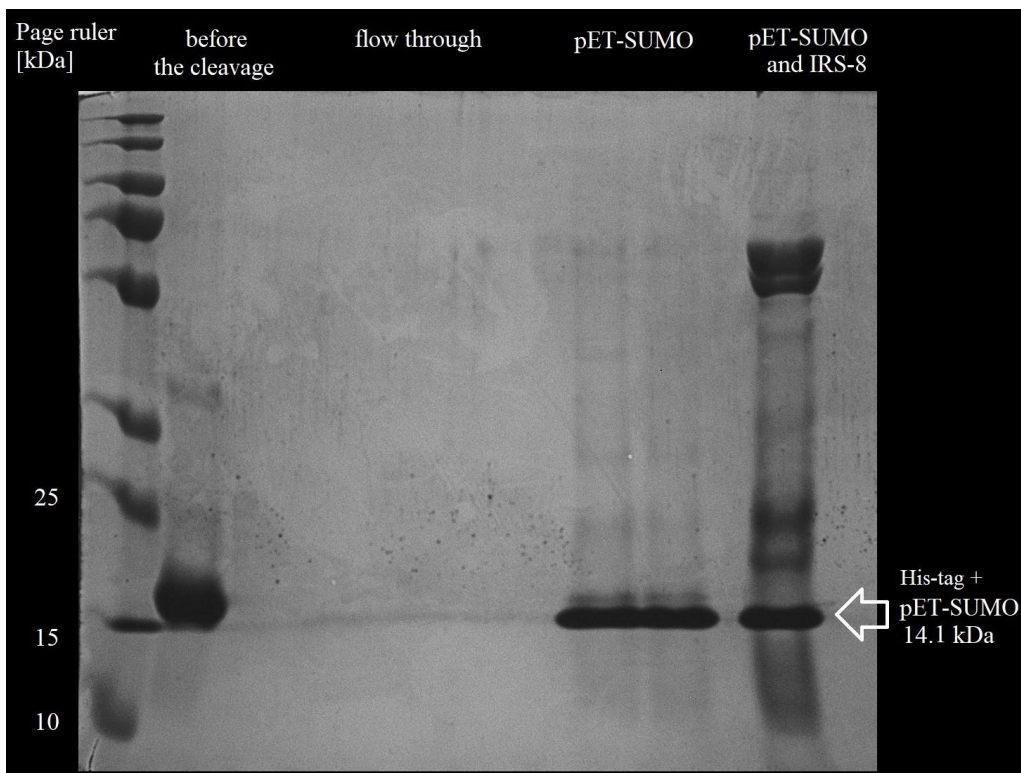


Figure 22: Second affinity chromatography. In the wells representing flow through the TIL-1 protein was not eluted. On the contrary, pET-SUMO was eluted from the column with 20 mM imidazole. To compare single pET-SUMO tag molecular weight and pET-SUMO TIL-1 complex in the sample, I used pET-SUMO tag cleft from IRS-8 (provided by Mgr. Kotál)

According to the second affinity chromatography result, I deduced that the pET-SUMO tag must have remained attached to the TIL-1 protein. Moreover, in spite of many optimizations of the cleavage conditions, removing the His-SUMO tag was not successfully performed.

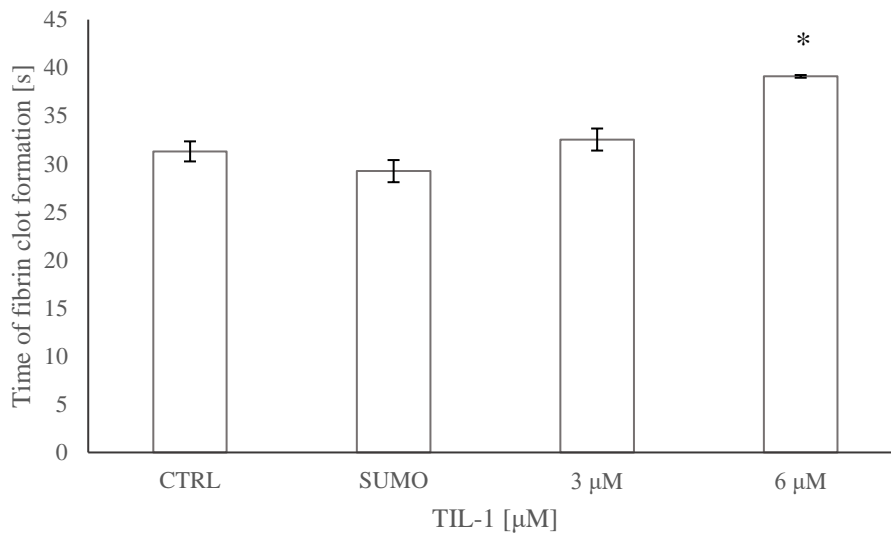
Nevertheless, I performed further assays with the TIL-1 -SUMO fusion protein and with the SUMO-tag as a control.

4.4 Coagulation assays

Before the coagulation assays, I calculated the concentrations of tested molecules using Bradford Albumin calibration curve from Pierce BCA protein assay kit (ThermoFischer Scientific). The molecule composed of TIL-1 attached to the pET-SUMO tag had 12.6 mg/ml, which corresponds to 540 μ M. pET-SUMO was 5.4 mg/ml corresponding to 405 μ M.

4.4.1 aPTT

As a first coagulation assay, I performed Activated Partial Thromboplastin Time (aPTT) starting with 6 μM of TIL-1 (in complex with pET-SUMO tag). Since the protein exhibited inhibition of fibrin clot formation, I lowered the concentration of TIL-1 protein to 3 μM . At the same time, I tested the previously isolated pET-SUMO molecule (at 6 μM) for its possible inhibitory activity. The results from aPTT were summarized in Graph 1 below.

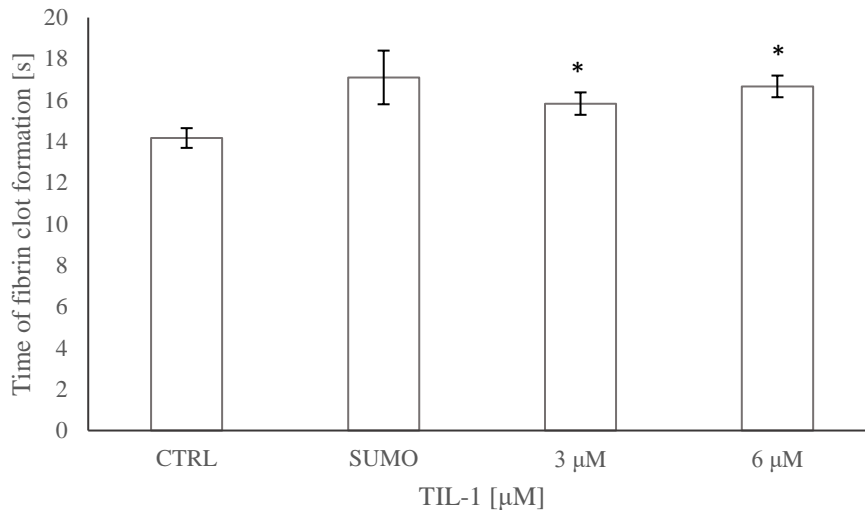


Graph 1: Effect of TIL-1 inhibitor and pET-SUMO tag on Activated Partial Thromboplastin Time; CTRL- a control of normal plasma coagulation without an inhibitor. According to Student's *t*-test, plasma coagulation inhibition was statistically significant with TIL-1 at 6 μM , whereas the inhibitory activity of 3 μM TIL-1 and 6 μM SUMO tag was not statistically significant. * $p < 0.05$

From Graph 1, it is evident that 6 μM TIL-1 protein inhibited plasma coagulation the most significantly. Student's *t*-test statistically proved the significance of inhibition of plasma coagulation. In comparison to the control plasma coagulation (CTRL), the time delay took 7.8 s.

4.4.2PT

In Prothrombin Time (PT) assay, no significant inhibition of plasma coagulation was observed, as shown in Graph 2.



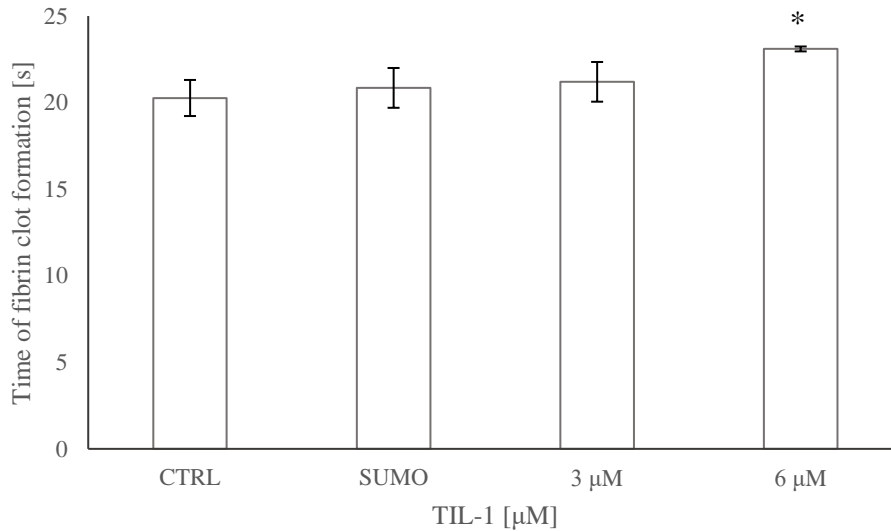
Graph 2: Effect of TIL-1 inhibitor and pET-SUMO tag on Prothrombin Time, CTRL- control of normal plasma coagulation without an inhibitor. According to the *t*-test, weak inhibition of fibrin clot formation was statistically significant using TIL-1 inhibitor at both 3 and 6 μM concentration.

* $p < 0.05$

According to the *t*-test, weak inhibition of fibrin clot formation with 6 and 3 μM TIL-1 (prolongation by 2.5 s and 1.6 s, respectively) was statistically significant. Conversely, the longest delay from the control coagulation was seen in the sample with the SUMO tag, which was not statistically significant.

4.4.3 TT

The Thromboplastin Time (TT) assay showed only a small inhibition effect of 6 μM TIL-1 protein (delay from the control plasma was 2.8 s), as shown in Graph 3.

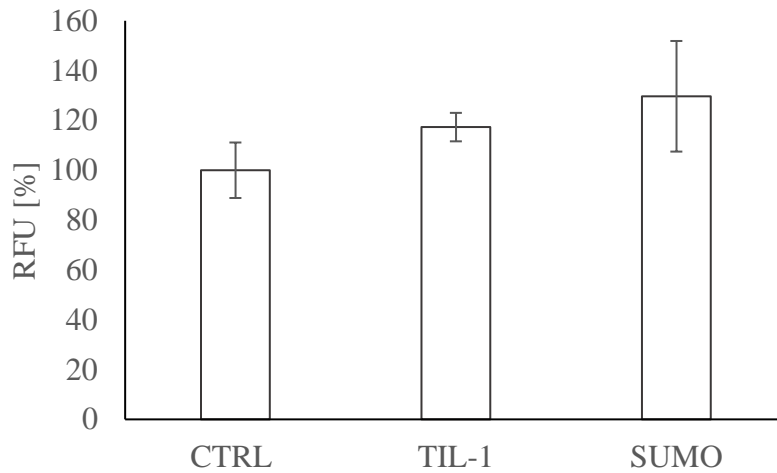


Graph 3: Effect of TIL-1 inhibitor and pET-SUMO tag on Thromboplastin Time, CTRL- control of normal plasma coagulation without an inhibitor. According to the *t*-test, weak inhibition of plasma coagulation was statistically significant only with TIL-1 at 6 μM . * $p < 0.05$

As expected, the lower concentration of TIL-1 protein showed negligible inhibition. The pET-SUMO tag did not inhibit the clot formation in this assay. Results of inhibition of 3 μM TIL-1 protein and the tag were not statistically significant.

4.5 Thrombin assay

The results from the thrombin assay are summarized in Graph 4 below. In this assay, I did not see any statistically significant thrombin inhibition by TIL-1 or SUMO tag.

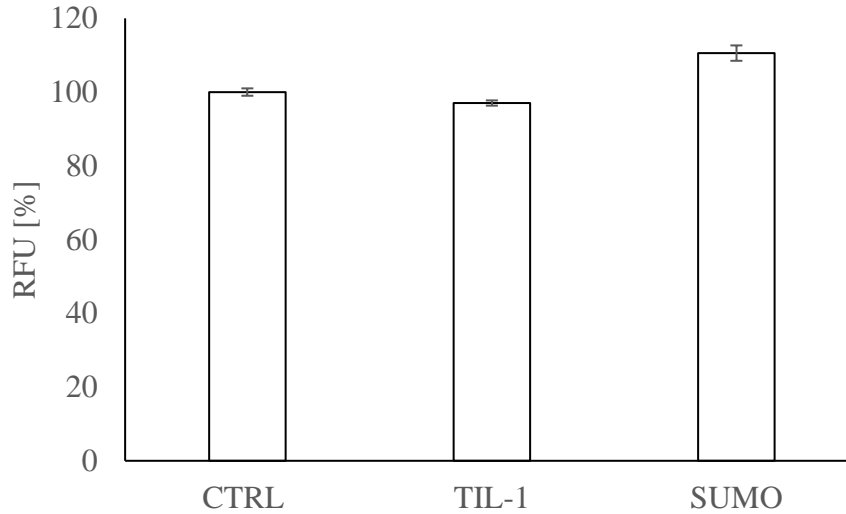


Graph 4: Effect of TIL-1 protein on thrombin binding to the fluorescent substrate. No inhibitory activity of thrombin-substrate binding of 5 μ M TIL-1 and 5 μ M SUMO tag was observed. RFU- relative fluorescence unit determined as the slope of regression line normalized to control group, where enzymatic activity was 100%, CTRL- control without inhibitor

According to the thrombin assay data, it is evident that TIL-1 protein most probably did not compete with the fluorescent substrate when binding with thrombin. According to the *t*-test, no statistically significant inhibition of thrombin was assumed.

4.6 Trypsin assay

The effect of TIL-1 protein on trypsin is outlined in Graph 5 below.



Graph 5: Effect of TIL-1 protein on trypsin proteolytic activity. According to the *t*-test, no statistically significant trypsin inhibition was observed with 5 μ M TIL-1, neither with 5 μ M SUMO. RFU-relative fluorescent unit determined as the slope of regression line normalized to control group, where enzymatic activity was 100%, CTRL- control without inhibitor

According to Graph 5, it is obvious that TIL-1 did not inhibit the trypsin. SUMO tag itself did not compete with the fluorescent substrate when binding to the trypsin. According to the *t*-test, the results are not statistically significant.

4.7 Purification of TIL-1 inhibitor from LPS

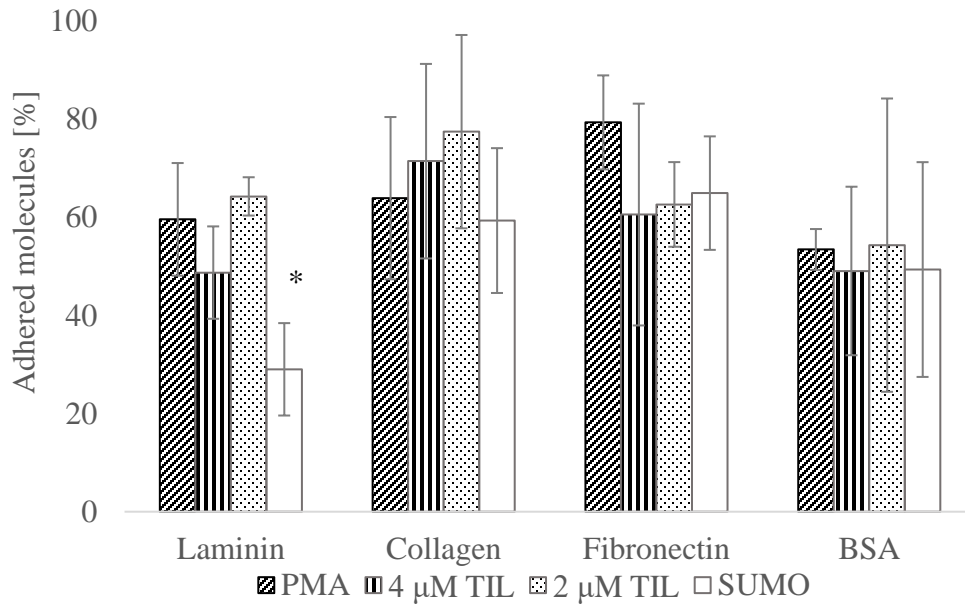
The samples containing the tag-protein complex and the sample containing only the pET-SUMO tag were purified from the excessing LPS with ToxinEraser Endotoxin Removal Kit (GenScript). The concentrations of LPS in samples were measured with PyroGene Recombinant Factor C Endotoxin Detection Assay (Lonza) before and after the purification and the concentrations of tag-protein complex and tag molecule were measured using Bradford Albumin calibration curve from Pierce BCA protein assay kit (ThermoFischer Scientific). The calculated values are summarized in Table 8.

BCA assay	Initial concentration [μM]	Final concentration [μM]	Recovery [%]
TIL-1	540.0	54.60	10.11
pET-SUMO	404.7	37.11	9.17
LPS removal assay	Initial concentration [EU/ml]	Final concentration [EU/ml]	
TIL-1	>10 *	0.154	
pET-SUMO	>10 *	0.013	

Table 8: Concentrations of TIL-1-pET-SUMO complex (TIL-1) and pET-SUMO, before and after the removal of LPS. Levels of LPS before and after using ToxinEraser Endotoxin Removal Kit (GenScript). *The initial concentration of LPS in samples was too high to be detected by the PyroGene Recombinant Factor C Endotoxin Detection Assay (Lonza) in plate reader Synergy H1 microplate reader (BioTek, Winooski, USA)

4.8 Monocyte adhesion

The monocyte adhesion results are summarized in Graph 6.



Graph 6: Adhesion of monocytes incubated with TIL-1 inhibitor (4 and 2 μ M) and pET-SUMO tag (4 μ M, marked as 'SUMO') to proteins of the extracellular matrix. PMA (Phorbol 12-myristate 13-acetate) represents a control group of normal activation of monocytes adhesion (absence of inhibitors). According to the *t*-test, inhibition of monocyte adhesion was statistically significant only on laminin. Unexpectedly, this inhibition was caused by SUMO-tag. The inhibition of adhesion was also observed on fibronectin. However, the *t*-test did not prove the inhibition statistically. BSA-bovine serum albumin used as a control of no adhesion on BSA blocked wells, * $p < 0.05$

From Graph 6, it is visible that the fluorescence measurement generated large standard deviations. The large error bars were probably mainly caused by the inconsistent portioning of monocytes in single wells.

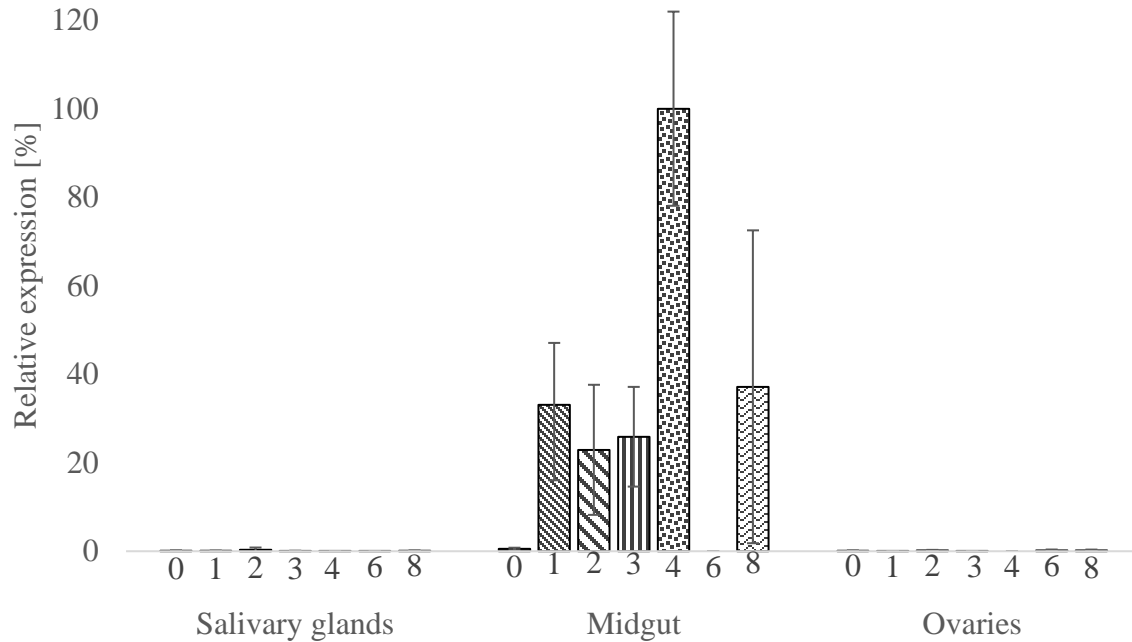
Inhibition of monocyte adhesion was observed mainly on laminin. However, the Student's *t*-test proved the statistical significance of the inhibition of SUMO-tag only. This effect, nevertheless, does not elucidate the function of the TIL-1 protein.

Although we could see an inhibitory trend in wells coated with fibronectin, according to the *t*-test, monocyte adhesion inhibition was not statistically significant. Surprisingly, a weak inhibitory effect on monocyte adhesion was observed again with SUMO-tag. Again, this does not give us any information about the potential immunomodulatory properties of TIL-1 protein, which could have potentially been caused by the tag itself and not TIL-1.

Wells coated only with 3 % BSA molecules were used as a control where the adhesion was not supposed to take place. Instead, the opposite effect was observed since the monocytes probably adhered to BSA. Therefore, it is possible that the actual adhesion may be a difference between proteins of the extracellular matrix and BSA.

4.9 qPCR

The tissue expression profile of TIL-1 is shown in Graph 7 below.



Graph 7: The tissue expression profile of TIL-1 in different tissues of unfed (day 0) and fed (day 1-8) adult female tick *I. ricinus*. The most significant expression was in the tick midgut.

Unfortunately, in this experiment, RNA from the midgut on the sixth day and ovaries on the fourth day of feeding was not successfully isolated in required biological triplications. Hence, the relative expression percentage in those days and tissues are missing in the results.

Nevertheless, according to the real-time PCR data, the relative expression of TIL-1 protein was most noticeable in the tick midgut.

The selected TIL-1 protein was initially revealed by RNA sequencing of the midgut from blood- and serum-fed *I. ricinus* (GenBank: GEFM01005205.1; Perner et al., 2016b). From the tissue expression profile results, it is obvious that the TIL-1 protein is synthesized in midgut in almost all tick blood-feeding stages.

5 Discussion

The actual structure of the TIL-1 protein was not resolved in this thesis. The sequence composition, nevertheless, suggests that it belongs to the TIL-domain family characteristic by serine protease inhibition. TIL-domain (including TIL-1 protein) typically contains a conserved core composed of 10 cysteines forming 5 disulfide bridges (Huang et al., 1994; Bania *et al.*, 1999). TIL-1 protein is likely to be a serine protease inhibitor with an exposed binding loop highly similar to all known TIL-domain inhibitor structures (Huang et al., 1994; Cierpicki et al., 2000; Bode and Huber 2000; Sasaki et al., 2008).

The protein structure prediction by Swiss model revealed the putative structure of TIL-1 protein. However, the position of the inhibitory RCL, the P1 site, occurred variable in respect to the mustel protein structure.

According to *A. mellifera* chymotrypsin inhibitor AMCI (PDB: 1ccv), the TIL-1 protein structure prediction should expose the inhibitory loop between 5th and 6th cysteine residue, at Met41 position (similar to AMCI with P1 at Met30; Cierpicki et al., 2000). The inhibitory loop of honeybee AMCI with P1 at Met30 strongly interacted with chymotrypsin and cathepsin G (Bania et al., 1999; Cierpicki et al., 2000).

In the TIL-1 protein structure prediction according to *Ascaris* chymotrypsin/elastase inhibitor (PDB: 1eai), the P1 binding site was expected at position Leu 31, as shown by Huang and colleagues (Huang et al., 1994). In the predictory structure of TIL-1, the leucine residue is neither exposed by the inhibitory loop, nor the RCL resides between 5th and 6th cysteine residues. Therefore, the position at Met41 in the model structure according to *Ascaris* TIL-domain inhibitor would be a more probable option. Because the P1 sites of the model and the mustel molecules do not match, I cannot affirm the putative function of the inhibitory loop in this model structure.

Similarly, the model structure that was built based on TIL-domain peptide from *B. bombina* BSTI (PDB:1hx2) showed a difference in the active site P1, which was predicted at Met41 (different to *B. bombina* with P1 at Glu32) (Rosengren et al., 2001). Therefore, no specific function of the predicted P1 site can be claimed here.

Protein structure prediction obtained from LOMETS missed the information of α -helices or β -sheets. Therefore, I could not analyze the structures more properly in Chimera software. Anyway, only one model structure, built according to honeybee TIL-domain inhibitor AMCI (PDB: 1ccv), exposed its binding loop in the expected position at Met30 (Cierpicki et al., 2000).

Two other model structures (according to frog TIL-domain inhibitor BSTI (PDB: 1hx2) and *Ascaris* TIL-domain inhibitor (PDB: 1eai)) did not possess binding loops at the correct positions (both at Lys32 instead of Leu31 and Glu32) (Rosengren et al., 2001; Huang et al., 1994).

According to the six predicted TIL-1 protein structures, the position of the P1 site seems variable. Nevertheless, I expect that the P1 site resembles between 5th and 6th cysteine residue (Huang et al., 1994; Bania et al., 1999), at the position between 30th and 41st residue of the protein structure. The purification of TIL-1 protein was efficient by the Nickel-Affinity chromatography. I needed only one affinity chromatography to get rid of the non-specifically expressed proteins and other impurities. The high purity of recombinant TIL-1 was caused mainly thanks to the His-SUMO fusion tag attached to the TIL-1 protein. Hence, the SUMO tag was useful in purification. The cleavage of the tag was, nevertheless, a tough nut to crack.

In comparison to the efficacy of expression and purification of untagged protein, using the SUMO tag was reasonable because of its simplicity and almost universal usage. The SUMO tag includes a polyhistidine tag and creates a covalent bond with a target protein, mostly at Lys residue. This bond is readily cleaved by SUMO protease. Moreover, SUMO tag usage increases protein expression and solubility (Yan et al., 2009; Kimple et al., 2013).

The untagged proteins usually require a multistep purification protocol (Figueiredo et al., 2016). Moreover, the usage of detergents might lead to protein precipitation, loss of the product or the protein aggregation and inclusion bodies formation (Figueiredo et al., 2016; Palmer and Wingfield 2004). The recovery of the protein from the inclusion bodies requires detergents such as urea, guanidine HCl, Triton X-100, organic acids, etc. (Palmer and Wingfield 2004; Wingfield, 2015). Once using the detergents for protein purification, they have to be removed by additional purification steps, such as guanidine HCl with reversed-phase chromatography (Wingfield et al., 1997, 2004). The formation of inclusion bodies and the usage of detergents might result in protein

degradation through incorrect folding, which corresponds to the loss of native protein function (Wingfield, 2015). Therefore, the challenge of purification of untagged proteins is not to efficiently purify them but to fold them into their native and active state (Wingfield, 2015). Thus, the SUMO tag usage was the preferred choice for the expression and purification of the novel recombinant TIL-1 protein from *I. ricinus*.

Coagulation assays were performed in order to verify the putative inhibitory effect on the coagulation cascade. On the one hand, in aPTT, plasma coagulation was inhibited by 6 μ M TIL-1 protein. The TT showed only a weak inhibitory effect of 6 μ M TIL-1, and PT results show almost negligible inhibition of 3 and 6 μ M TIL-1. On the other hand, the SUMO tag itself did not show statistically significant fibrin clot formation inhibition. That might indicate that the TIL-1 protein can inhibit some serine protease factors present in the intrinsic coagulation pathway.

The anti-hemostatic properties of tick serine protease inhibitors seem beneficial for the parasite. Ticks and other blood-feeding animals need to retain the blood fluid to easily digest it (Schwarz et al., 2014). To date, there are no anti-coagulation properties described in TIL-domains of other ticks. Compared to other serine protease inhibitors from ticks, e.g., Kunitz-domain inhibitor rBmTI-A, whose transcripts are mainly expressed in the tick midgut, strongly inhibited the common coagulation pathway by targeting trypsin, plasmin, hNE, and plasma kallikrein (Tanaka et al., 1999; Soares et al., 2016). The rBmTI-A inhibitor could, therefore, play a crucial role in controlling blood coagulation, inflammation, and angiogenesis during the larval feeding process (Soares et al., 2016).

The possibility of inhibiting common coagulation pathway (thrombin triggering the formation of fibrin clot) was declined both by Thromboplastin Time and Thrombin assay itself.

The anti-coagulation properties were described in proteins with the TIL-domain in the hematophagous nematodes *Ancylostoma caninum* (Stassens et al., 1996). In the nematode, the TIL-domain inhibitor serves to block blood coagulation factor Xa (fXa) and coagulation factor VIIa and tissue factor (fVIIa/TF). Therefore, TIL-domain peptides from nematode *A. caninum* inhibits extrinsic and common coagulation pathways (Stassens et al., 1996). The common

coagulation pathway was hindered by the isolates of the frog *B. bombina* skin by inhibiting thrombin activity (Mignogna et al., 1996).

From the trypsin assay, it is evident that there was no inhibition of trypsin proteolytic activity. I expect that this might have been caused by the fact that the P1 site of the TIL-1 protein was hidden within the large SUMO tag. Therefore, the P1 of TIL-1 could not be exposed and bind the trypsin. The same might be valid for thrombin.

Anyway, the serine protease inhibitory properties of TIL-domain peptides seem highly variable among different species. There are only a few TIL-domain proteins from ticks with resolved anti-protease properties to the best of my knowledge. A TIL-domain inhibitor Ixodidin from *R. microplus* exerts inhibitory activity against elastase and chymotrypsin (Fogaca et al., 2006). Another TIL-domain inhibitor isolated from *R. microplus*, BmSIs inhibited subtilisin A, hNE, fungal protease Pr1, but trypsin nor thrombin (Sasaki et al., 2008).

Unlike TIL-1 from *I. ricinus*, in the TIL-domain containing BSTI peptide from skin secretions of the frog *B. bombina*, the activity of trypsin and thrombin was blocked (Mignogna et al., 1996). The BSTI anti-protease function might be used to prevent premature liberation or degradation of skin peptides in frog's skin (Mignogna et al., 1996). Using TIL-domain peptides from *L. laevis* in proteolytic assays, the inhibition was shown only with trypsin (Wang et al., 2015). The venom serine protease inhibitor (AcVSPI) isolated from honeybee *A. cerana* showed inhibitory activity against fungal growth, a microbial serine protease, trypsin, and plasmin (Yang et al., 2017). On the contrary, the AMCI inhibitor isolated from the honeybee *A. mellifera* showed anti-proteolytic activity against bovine chymotrypsin, but not against trypsin nor thrombin (Bania et al., 1999). The honeybees utilize the serine protease inhibitor as a low-molecular-weight allergen in its venom. (Michel et al., 2012).

The monocyte adhesion experiment results did not show the immunomodulatory properties of TIL-1 protein, common for salivary protease inhibitors, which confirms our data about its localization mainly in tick midgut. Quite oppositely, weak inhibition of monocyte adhesion was observed with SUMO-tag. However, this does not provide us with any information about possible other immunomodulatory properties of TIL-1 protein. The modulation of the host immune

response was shown with TIL-domain inhibitor from *R. microplus* (BmSI 7), which regulated bovine neutrophil elastase pro-inflammatory activity (Sasaki et al. 2008). Other tick serine protease inhibitors showed more vertebrate host-immune modulation, like Kunitz-domain inhibitors, e.g., rBmTIs (Sasaki et al., 2004) and serpins, e.g., IRS-2 (Chmelar et al., 2012). It's given by the fact that these protein groups are generally more often studied from different perspectives.

The qPCR revealed the relative expression of TIL-1 protein most significantly in the tick midgut. qPCR confirmed that the TIL-1 sequence found under GenBank accession number GEFM01005205.1 originates from the *I. ricinus* midgut (Perner et al., 2016b).

The TIL-1 inhibitor was synthesized in almost all stages of blood-sucking adult female tick in its midgut. Since ticks require a blood meal to develop and reproduce successfully, they necessitate effective blood uptake and digestion mechanisms. In several studies, midgut transcriptome (mialome) analyses show several enzymes associated with protein, carbohydrate, and lipid digestion that could be related to tick blood uptake, prevention of blood coagulation, and blood digestion (Schwarz et al., 2014; Kotsyfakis et al., 2015a; Perner et al., 2016). Especially TIL-domain peptides, Kunitz-domain peptides, cystatins, and serpins are expressed 1 000 times more in the midgut than in salivary glands (Kotsyfakis et al., 2015a). According to the qPCR results and the coagulation assays, the TIL-1 protein could prevent the sucked blood from aggregating in the midgut and help the tick digest the blood meal.

6 Conclusion

A novel *I. ricinus* TIL-domain inhibitor named TIL-1 was presented in this thesis. The TIL-domain family of *I. ricinus* was analyzed *in silico*, including phylogenetic clustering and the protein structure predictions. The selected TIL-1 protein was cloned, and the recombinant TIL-1 inhibitor was successfully expressed and purified by affinity chromatography. The TIL-1 inhibitor attached to the His-SUMO tag was tested for its biochemical, anticoagulation, and immunomodulatory properties. The tissue expression profile of TIL-1 in a tick was shown by qPCR in various tick feeding stages.

The elucidation of the exact protein structure would help reveal the mechanism of binding to the serine proteases and the coagulation inhibition background. Here we created 17 TIL-domain inhibitor groups *in silico*, which deserve to be cloned, produced recombinantly, and analyzed in order to reveal their possible anticoagulation, immunomodulatory, and even antimicrobial properties.

7 References

- Allan, L. A., and Clarke, P. R.** (2009). Apoptosis and autophagy: Regulation of caspase-9 by phosphorylation. *FEBS J.* 276, 6063e6073.
- Altschul, S. F., Madden, T. L., Schäffer, A. A., Zhang, J., Zhang, Z., Miller, W., and Lipman, D. J.** (1997). Gapped BLAST and PSI-BLAST: A new generation of protein database search programs, *Nucleic Acids Res.* 25, 3389-3402.
- Augustin, R., Siebert, S., and Bosch, T.C.** (2009). Identification of a Kazal-type serine protease inhibitor with potent anti-staphylococcal activity as part of Hydra's innate immune system. *Dev. Comp. Immunol.* 33, 830e837.
- Bania, J., Stachowiak, D., and Polanowski, A.** (1999). Primary structure and properties of the cathepsin G/chymotrypsin inhibitor from the larval hemolymph of *Apis mellifera*. *Eur. J. Biochem.* 262, 680–687.
- Benkert, P., Biasini, M., and Schwede, T.** (2011). Toward the estimation of the absolute quality of individual protein structure models. *Bioinformatics* 27, 343-350.
- Bernard, V. D., and Peanasky, R. J.** (1993). The serine protease inhibitor family from *Ascaris suum*: Chemical determination of the five disulfide bridges. *Arch Biochem Biophys.* 303(2), 367-76.
- Bertoni, M., Kiefer, F., Biasini, M., Bordoli, L., and Schwede, T.** (2017). Modeling protein quaternary structure of homo- and hetero-oligomers beyond binary interactions by homology. *Sci. Rep.* 7(1), 10480.
- Bienert, S., Waterhouse, A., de Beer, T.A.P., Tauriello, G., Studer, G., Bordoli, L., and Schwede, T.** (2017). The SWISS-MODEL Repository - new features and functionality. *Nucleic Acids Res.* 45, D313-D319.
- Birk, Y., Gertler, A., and Khalef, S.** (1967). Further evidence for a dual, independent, activity against trypsin and alpha-chymotrypsin of inhibitor AA from soybeans. *Biochim Biophys Acta* 147(2), 402-4.

- Blisnick, A. A., Foulon, T., and Bonnet, S. I.** (2017) Serine protease inhibitors in ticks: An overview of their role in tick biology and tick-borne pathogen transmission. *Front. Cell. Infect. Microbiol.* 7:199.
- Bode, W. and Huber, R.** (2000). Structural basis of the endoproteinase-protein inhibitor interaction. *Biochim. Biophys. Acta* 1477, 241-252.
- Brossard, M., and Wikel, S. K.** (2004). Tick immunobiology. *Parasitology* 129(Suppl.), S161–S176.
- Camacho, C., Coulouris, G., Avagyan, V., Ma, N., Papadopoulos, J., Bealer, K., and Madden, T.L.** (2009). BLAST+: Architecture and applications. *BMC Bioinformatics* 10, 421-430.
- Carrell, R. W., and Read, R. J.** (2016). How serpins transport hormones and regulate their release. *Semin. Cell Dev. Biol.* 62, 133–141.
- Carrel, R. W., and Travis, J.** (1985). α_1 -antitrypsin and the serpins. Variation and conservation. *Trends Biol. Sci.* 10, 20-24.
- Caughey, G. H.** (2016). Mast cell proteases as pharmacological targets. *Eur. J. Pharmacol.* 778, 44–55.
- Cerenius, L., Liu, H., Zhang, Y., Rimphanitchayakit, V., Tassanakajon, A., Gunnar Andersson, M., et al.** (2010). High sequence variability among hemocytespecific Kazal-type proteinase inhibitors in decapod crustaceans. *Dev. Comp. Immunol.* 34, 69–75.
- Ceuleers, H., Hanning, N., Heirbaut, J., Van Remoortel, S., Joossens, J., Van Der Veken, P., Francque, S. M., De Bruyn, M., Lambeir, A. M., De Man, J. G., Timmermans, J. P., Augustyns, K., De Meester, I., De Winter, B. Y.** (2018). Newly developed serine protease inhibitors decrease visceral hypersensitivity in a post-inflammatory rat model for irritable bowel syndrome. *Br J Pharmacol.* 175(17), 3516-3533.
- Chmelar, J., Calvo, E., Pedra, J. H., Francischetti, I. M., and Kotsyfakis, M.** (2012). Tick salivary secretion as a source of antihemostatics. *J. Proteomics* 75, 3842–3854.

Chmelar, J., Kotal, J., Karim, S., Kopacek, P., Francischetti, I. M., Pedra, J. H., and Kotsyfakis, M. (2016). Sialomes and mialomes: A systems-biology view of tick tissues and tick host interactions. *Trends in parasitology* 32(3), 242-254.

Chmelar, J., Kotál, J., Kovariková, A., and Kotsyfakis, M. (2019). The use of tick salivary proteins as novel therapeutics. *Front. Physiol.* 10:812.

Chmelar, J., Kotál, J., Langhansová, H., and Kotsyfakis, M. (2017). Protease inhibitors in tick saliva: The role of serpins and cystatins in tick-host-pathogen interaction. *Front. Cell. Infect. Microbiol.* 7:216.

Chmelar, J., Oliveira, C. J., Rezacova, P., Francischetti, I. M., Kovarova, Z., Pejler, G., et al. (2011). A tick salivary protein targets cathepsin G and chymase and inhibits host inflammation and platelet aggregation. *Blood* 117, 736–744.

Cierpicki, T., Bania, J., and Otlewski, J., (2000). NMR solution structure of *Apis mellifera* chymotrypsin/cathepsin G inhibitor-1 (AMCI-1): Structural similarity with *Ascaris* protease inhibitors. *Protein Sci.* 9, 976–984.

Corral-Rodriguez, M. A., Macedo-Ribeiro, S., Barbosa Pereira, P. J., and Fuentes-Prior, P. (2009). Tick-derived Kunitz-type inhibitors as antihemostatic factors. *Insect. Biochem. Mol. Biol.* 39, 579–595.

Costantino, C. M., Ploegh, H. L., and Hafler, D. A. (2009). Cathepsin S regulates class II MHC processing in human CD4 β HLA-DR β T cells. *J. Immunol.* 183, 945e952.

Crocetti, L., Quinn, M. T., Schepetkin, I. A., and Giovannoni, M. P. (2019). A patenting perspective on human neutrophil elastase (HNE) inhibitors (2014-2018) and their therapeutic applications. *Expert Opin Ther Pat.* 7, 555-578.

Cuervo, A. M., and Dice, J.F. (1998) Lysosomes, a meeting point of proteins, chaperones, and proteases. *J. Mol. Med.* 76, 6e12.

De Paula, V. S., Sgourakis, N. G., Francischetti, I. M., Almeida, F. C. L., Monteiro, R. Q., Valente, A. P. (2019). NMR structure determination of Ixolaris and factor X(a) interaction reveals a noncanonical mechanism of Kunitz inhibition. *Blood* 134(8), 699–708.

De Veer, S.J., Furio, L., Harris, J.M., et al. (2014). Proteases: Common culprits in human skin disorders. *Trends Mol Med.* 20(3), 166–178.

Drag, M., and Salvesen, G.S. (2010). Emerging principles in protease-based drug discovery. *Nat Rev Drug Discov.*;9(9), 690–701.

Dehghani, M., Kazemi Shariat Panahi, H., Holmes, E. C., Hudson, B. J., Schloeffel, R., and Guillemin, G. J. (2019). Human tick-borne diseases in Australia. *Front. Cell Infect. Microbiol.* 9, 3.

Eapen, M. S., Myers, S., Walters, E. H., et al. (2017) Airway inflammation in chronic obstructive pulmonary disease (COPD): A true paradox. *Expert Rev Respir Med.* 11, 827–839.

Figueiredo, D. B., Carvalho, E., Santos, M. P., Kraschowetz S., Zanardo, R. T., Campani Jr., G., Silva, G. G., Sargo, C. R., Horta, A. C. L., de C. Giordano, R., Miyaji, E. N., Zangirolami, T. C., Cabrera-Crespo, J., and Gonçalves, V. M. (2017). Production and purification of an untagged recombinant pneumococcal surface protein A (PspA4Pro) with high-purity and low endotoxin content. *Appl Microbiol Biotechnol* 101, 2305–2317.

Florencio, A. C., de Almeida, R. S., Arantes-Costa, F. M., Saraiva-Romanholo, B.M., Duran, A. F., Sasaki, S. D., Martins, M. A., Lopes, F. D. T. Q. S., Tibério, I. F. L. C., and Leick, E.A. (2019). Effects of the serine protease inhibitor rBmTI-A in an experimental mouse model of chronic allergic pulmonary inflammation. *Sci Rep.* 9(1), 12624.

Fogaca, A. C., Almeida, I. C., Eberlin, M. N., Tanaka, A. S., Bulet, P., and Daffre, S. (2006). Ixodidin, a novel antimicrobial peptide from the hemocytes of the cattle tick *Boophilus microplus* with inhibitory activity against serine proteinases. *Peptides* 27, 667–674.

Francischetti, I. M., Valenzuela, J. G., Andersen, J. F., Mather, T. N., and Ribeiro, J. M. (2002). Ixolaris, a novel recombinant tissue factor pathway inhibitor (TFPI) from the salivary gland of the tick, *Ixodes scapularis*: Identification of factor X and factor Xa as scaffolds for the inhibition of factor VIIa/tissue factor complex. *Blood* 99(10), 3602–3612.

- Fullaondo, A., García-Sánchez, S., Sanz-Parra, A., Recio, E., Lee, S. Y., and Gubb, D.** (2011). Spn1 regulates the GNBP3-dependent Toll signaling pathway in *Drosophila melanogaster*. *Mol Cell Biol.* 31(14), 2960-72.
- Gettins, P. G. W.** (2000). Keeping the serpin machine running smoothly. *Genome Res.* 10, 1833-1835.
- Gettins, P. G. W., Patston, P. A., and Olson, S. T.** (1996). Serpins: Structure, function and biology, molecular biology intelligence unit, Landes R. G. et al. and *Chapman & Hall, Austin, TX.*
- Giachetto, P. F., Cunha, R. C., Nhani, A. Jr., Garcia, M. V., Ferro, J. A., and Andreotti, R.** (2020). Gene expression in the salivary gland of *Rhipicephalus (Boophilus) microplus* fed on tick-susceptible and tick-resistant hosts. *Front. Cell. Infect. Microbiol.* 9, 477.
- Grover, S. P., and Mackman, N.** (2018). Tissue factor: an essential mediator of hemostasis and trigger of thrombosis. *Arterioscler Thromb Vasc Biol.* 38(4), 709-725.
- Gu, Q., Zhou, S., Zhou, Y., Huang, J., Shi, M., and Chen, S.** (2019). A trypsin inhibitor-like protein secreted by *Cotesia vestalis* teratocytes inhibits hemolymph prophenoloxidase activation of *Plutella xylostella*, *Journal of Insect Physiology.* 116, 41-48.
- Guex, N., Peitsch, M.C., and Schwede, T.** (2009). Automated comparative protein structure modeling with SWISS-MODEL and Swiss-PdbViewer: A historical perspective. *Electrophoresis* 30, S162-S173.
- Guttman-Yassky, E., Krueger, J. G., and Lebwohl, M. G.** (2017). Systemic immune mechanisms in atopic dermatitis and psoriasis with implications for treatment. *Exp Dermatol.* 27, 409-417.
- Hall, T. A.** (1999). BioEdit: A user-friendly biological sequence alignment editor and analysis program for Windows 95/98/NT. *Nucl. Acids. Symp. Ser.* 41, 95-98.
- Han, N., Jin, K., He, K., Cao, J., and Teng, L.** (2011). Protease-activated receptors in cancer: A systematic review. *Oncol. Lett.* 2, 599–608.

- Hartl, M., Giri, A. P., Kaur H., and Baldwin, I. T.** (2011). The multiple functions of plant serine protease inhibitors: Defense against herbivores and beyond. *Plant Signal Behav.* 6, 1009–1011.
- Haynes, R., and Feeney, R. K.** (1967). Fractionation and properties of trypsin and chymotrypsin inhibitors from lima beans. *J Biol Chem.* 242(22), 5378-85.
- Hedstrom, L.** (2002). Serine protease mechanism and specificity. *Chem Rev.* 102(12), 4501–4524.
- Hemker, H. C., Willems, G. M., and Béguin, S.** (1986). A computer assisted method to obtain the prothrombin activation velocity in whole plasma independent of thrombin decay processes. *Thromb Haemost.* 56(1), 9-17.
- Huang, K., Strynadka, N. C., Bernard, V. D., Peanasky, R. J., and James, M. N.** (1994). The molecular structure of the complex of *Ascaris* chymotrypsin/elastase inhibitor with porcine elastase. *Structure* 2(7), 679-89.
- Huber, R. and Bode, W.** (1978). Structural basis of the activation and action of trypsin. *Acc. Chem. Res.* 11, 114-122.
- Hunt, T. L., and Dayhoff, M. O.** (1980). A surprising new protein superfamily containing ovalbumin, antithrombin III and α_1 -proteinase inhibitor. *Biochem. Biophys. Res. Commun.* 95, 864-871.
- Huntington, J. A., and Li, W.** (2009). Structural insights into the multiple functions of protein C inhibitor. *Cell. Mol. Life Sci.* 66, 113–121.
- Huntington, J. A., Read, R. J., and Carrell, R. W.** (2000). Structure of a serpin protease complex shows inhibition by deformation. *Nature* 407(6806), 923.
- Irving, J. A., Pike, R. N., Lesk, A. M., and Whisstock, J. C.** (2000). Phylogeny of the serpin superfamily: Implications of patterns of amino acid conservation for structure and function. *Genome research* 10(12), 1845-1864.

- Jouiaei, M., Casewell, N. R., Yanagihara, A. A., Nouwens, A., Cribb, B. W., and Whitehead, D.** (2015). Firing the sting: Chemically induced discharge of cnidae reveals novel proteins and peptides from box jellyfish (*Chironex fleckeri*) venom. *Toxins (Basel)* 7, 936–950.
- Johnson, D. J., and Huntington, J. A.** (2003). Crystal structure of antithrombin in a heparin-bound intermediate state. *Biochemistry* 42, 8712-8719.
- Kanost, M. R.** (1999). Serine proteinase inhibitors in arthropod immunity. *Dev. Comp. Immunol.* 23, 291–301.
- Kaslik, G., Patthy, A., Balint, M. and Graf, L.** (1995). Trypsin complexed with alpha 1-proteinase inhibitor has an increased structural flexibility. *FEBS Lett.* 370, 179-183.
- Kass, I., Reboul, C. F., and Buckle, A. M.** (2011). Chapter fourteen - Computational methods for studying serpin conformational change and structural plasticity. *Methods in Enzymology.* 501, 295-323.
- Kazal, L. A., Spicer, D. S., and Brahinsky, R. A.** (1948). Isolation of a crystalline trypsin inhibitor-anticoagulant protein from pancreas. *J Am Chem Soc.* 70(9), 3034-40.
- Kazimirova, M., Thangamani, S., Bartikova, P., Hermance, M., Holikova, V., Stibraniova, I., et al.** (2017). Tick-borne viruses and biological processes at the tick-host-virus interface. *Front. Cell Infect. Microbiol.* 7, 339.
- Kettritz, R.** (2016) Neutral serine proteases of neutrophils. *Immunol Rev.* 273(1), 232–248.
- Khan, A. R., and James, M.N.** (1998). Molecular mechanisms for the conversion of zymogens to active proteolytic enzymes. *Protein Sci.* 7, 815e836.
- Kimple, M. E., Brill, A. L., and Pasker, R. L.** (2013). Overview of affinity tags for protein purification. *Curr Protoc Protein Sci.* 73, 9.9.1–9.9.23.
- Korkmaz, B., Moreau, T., and Gauthier, F.** (2008). Neutrophil elastase, proteinase 3 and cathepsin G: Physicochemical properties, activity and physiopathological functions. *Biochimie* 90, 227e242.

- Kotsyfakis, M.** (2013). *De novo Ixodes ricinus* salivary gland transcriptome analysis using two next-generation sequencing methodologies. *The FASEB Journal* 27(12), 4745–4756.
- Kotsyfakis, M., Kopáček, P., Franta, Z., Pedra, J. H. F., and Ribeiro, J. M. C.** (2015b). Deep sequencing analysis of the *Ixodes ricinus* haemocytome. *PLoS Negl Trop Dis.* 9(5), e0003754.
- Kotsyfakis, M., Schwarz, A., Erhart, J., and Ribeiro, J. M. C.** (2015a). Tissue- and time-dependent transcription in *Ixodes ricinus* salivary glands and midguts when blood feeding on the vertebrate host. *Sci Rep.* 5, 9103.
- Kovarova, Z., Chmelar, J., Sanda, M., Brynda, J., Mares, M., and Rezacova, P.** (2010). Crystallization and diffraction analysis of the serpin IRS-2 from the hard tick *Ixodes ricinus*. *Acta Crystallogr. Sect. F Struct. Biol. Cryst. Commun.* 66, 1453–1457.
- Krantz, A.** (1992). A classification of enzyme inhibitors. *Bioorg Med Chem Lett.* 2(11), 1327–1334.
- Kumar, S., Stecher, G., and Tamura, K.** (2016). MEGA7: Molecular Evolutionary Genetics Analysis version 7.0 for bigger datasets. *Molecular Biology and Evolution* 33, 1870-1874.
- Kunitz, M.** (1945). Crystallization of a trypsin inhibitor from soybean. *Science* 101, 668–669.
- Kuwar, S. S., Pauchet, Y., Vogel, H., and Heckel, D. G.** (2015). Adaptive regulation of digestive serine proteases in the larval midgut of *Helicoverpa armigera* in response to a plant protease inhibitor. *Insect Biochem Mol Biol.* 59, 18-29.
- Langdell, R. D., Wagner, R. H., and Brinkhous, K. M.** (1953). Effect of antihemophilic factor on one-stage clotting tests; a presumptive test for hemophilia and a simple one-stage antihemophilic factor assay procedure. *J Lab Clin Med.* 41(4), 637–47.
- Law, R. H., Zhang, Q., McGowan, S., Buckle, A. M., Silverman, G. A., Wong, W., and Whisstock, J. C.** (2006). An overview of the serpin superfamily. *Genome biology* 7(5), 216.
- Leboulle, G., Crippa, M, Decrem, Y, et al.** (2002) Characterization of a novel salivary immunosuppressive protein from *Ixodes ricinus* ticks. *J Biol Chem.* 277(12), 10083-10089.

- Li, Y., Dong, Z., Liu, H., Zhu, R., Bai, Y., Xia, Q., and Zhao, P. (2018).** The fungal-resistance factors BmSPI38 and BmSPI39 predominantly exist as tetramers, not monomers, in *Bombyx mori*. *Insect Molecular Biology* 27(6), 686-697.
- Li, Y., Liu, H., Zhu, R., Xia, Q., and Zhao, P. (2016a).** Loss of second and sixth conserved cysteine residues from trypsin inhibitor-like cysteine-rich domain-type protease inhibitors in *Bombyx mori* may induce activity against microbial proteases. *Peptides* 86, 13–23.
- Li, J., Zhang, C., Xu, X., Wang, J., Yu, H., Lai, R. and Gong, W. (2007).** Trypsin inhibitory loop is an excellent lead structure to design serine protease inhibitors and antimicrobial peptides. *The FASEB Journal* 21, 2466-2473.
- Li, Y., Zhao, P., Liu, S., Dong, Z., Chen, J., Xiang, Z., and Xia, Q. (2012b).** A novel protease inhibitor in *Bombyx mori* is involved in defense against *Beauveria bassiana*. *Insect Biochem. Mol. Biol.* 42, 766e775.
- Li, Y., Zhao, P., Liu, H., Guo, X., He, H., Zhu, R., Xiang, Z., and Xia, Q. (2015).** TIL-type protease inhibitors may be used as targeted resistance factors to enhance silkworm defenses against invasive fungi. *Insect Biochemistry and Molecular Biology* 57, 11-19.
- Liang, G., and Bowen, J. P. (2016).** Development of trypsin-like serine protease inhibitors as therapeutic agents: Opportunities, challenges, and their unique structure-based rationales. *Curr Top Med Chem.* 16(13), 1506–1529.
- Lima, L. G., and Monteiro, R. Q. (2013).** Activation of blood coagulation in cancer: Implications for tumour progression. *Biosci. Rep.* 33, 10.
- Lineweaver, H., and Murray, C. W. (1947).** Identification of the trypsin inhibitor of egg white with ovomucoid. *J Biol Chem.* 171(2), 565–81.
- Liu, H., Chen, J., Wang, X., Yan, S., Xu, Y., and San, M. (2015).** Functional characterization of a new non-Kunitz serine protease inhibitor from the scorpion *Lychas mucronatus*. *Int J Biol Macromol.* 72, 158–162.

- López-Otín, C., and Bond, J. S.** (2008). Proteases: Multifunctional enzymes in life and disease. *The Journal of biological chemistry* 283(45), 30433–30437.
- Lourenço, J. D., Ito, J. T., Cervilha, D. A. B., Sales, D. S., Riani, A., Suehiro, C. L., Genaro, I. S., Duran, A., Puzer, L., Martins, M. A., Sasaki, S. D., and Lopes, F. D. T. Q. S.** (2018). The tick-derived rBmTI-A protease inhibitor attenuates the histological and functional changes induced by cigarette smoke exposure. *Histol Histopathol.* 33(3), 289-298.
- Maritz-Olivier, C., Stutzer, C., Jongejan, F., Neitz, A. W. H., and Gaspar, A. R. M.** (2007). Tick antihemostatics: Targets for future vaccines and therapeutics. *Trends Parasitol.* 23, 397–407.
- Michel, Y., McIntyre, M., Ginglinger, H., Ollert, M., Cifuentes, L., Blank, S., and Spillner, E.** (2012). The putative serine protease inhibitor Api m 6 from *Apis mellifera* venom: recombinant and structural evaluation. *J Investig Allergol Clin Immunol.* 22, 476–484.
- Mignogna, G., Pascarella, S., Wechselberger, C., Hinterleitner, C., Mollay, C., Amiconi, G., Barra, D., and Kreil, G.** (1996). BSTI, a trypsin inhibitor from skin secretions of *Bombina bombina* related to protease inhibitors of nematodes. *Protein Sci.* 5, 357–362.
- Miyata, J., Tani, K., Sato, K., Otsuka, S., Urata, T., Lkhagvaa, B., et al.** (2007). Cathepsin G: The significance in rheumatoid arthritis as a monocyte chemoattractant. *Rheumatol Int.* 27, 375–382.
- Molehin, A. J., Gobert, G. N., and McManus, D. P.** (2012). Serine protease inhibitors of parasitic helminths. *Parasitology* 139, 681–695.
- Murakami, Y., Wada, Y., Kobayashi, H., Irie, A., Hasegawa, M., and Yamanaka, H.** (2012). Inhibition of *Aeromonas sobria* serine protease (ASP) by α 2-macroglobulin. *Biol Chem.* 393, 1193–1200.
- Nagata, K.** (1996). Hsp47: a collagen-specific molecular chaperone. *Trends Biochem. Sci.* 21(1), 23-26.

- Nazareth, R. A., Tomaz, L. S., Ortiz-Costa, S., et al.** (2006). Antithrombotic properties of Ixolaris, a potent inhibitor of the extrinsic pathway of the coagulation cascade. *Thromb Haemost.* 96(1), 7-13.
- Negulescu, H., Guo, Y., Garner, T. P., Goodwin, O. Y., Henderson, G., and Laine, R. A.** (2015). A Kazal-type serine protease inhibitor from the defense gland secretion of the subterranean termite *Coptotermes formosanus shiraki*. *PLoS ONE.* 10, e0125376.
- Nielsen, H., Engelbrecht, J., Brunak, S., and von Heijne, G.** (1997). Identification of prokaryotic and eukaryotic signal peptides and prediction of their cleavage sites. *Prot. Eng.* 10, 1-6.
- Nuttall, P. A., and Labuda, M.** (2004). Tick-host interactions: saliva-activated transmission. *Parasitology* 129, S177–S189.
- Nuttall, P. A., and Labuda, M.** (2008). Saliva-assisted transmission of tick-borne pathogens, in *Ticks: Biology, Disease and Control*, eds Bowman, A. S., and Nuttall, P. A. (Cambridge: Cambridge University Press), 205–219.
- Ohmuraya, M., and Yamamura, K.** (2011). Roles of serine protease inhibitor Kazal type 1 (SPINK1) in pancreatic diseases. *Exp Anim.* 60, 433–444.
- Olson, S. T., Bock, P. E., Kvassman, J., Shore, J. D., Lawrence, D. A., Ginsburg, D., and Björk, I.** (1995). Role of the catalytic serine in the interactions of serine proteinases with protein inhibitors of the serpin family. Contribution of a covalent interaction to the binding energy of serpin-proteinase complexes. *J Biol Chem.* 270, 30007-30017.
- Page, M. J., and Di Cera, E.** (2008). Serine peptidases: Classification, structure and function. *Cell Mol Life Sci.* 65(7–8), 1220–1236.
- Palenikova, J., Lieskovska, J., Langhansova, H., Kotsyfakis, M., Chmelar, J., and Kopecky, J.** (2015). *Ixodes ricinus* salivary serpin IRS-2 affects Th17 differentiation via inhibition of the interleukin-6/STAT-3 signaling pathway. *Infect. Immun.* 83, 1949–1956.

- Palermo, C. J., and Joyce, A.** (2008). Cysteine cathepsin proteases as pharmacological targets in cancer. *Trends Pharmacol. Sci.* 29, 22e28.
- Palmer, I., and Wingfield, P. T.** (2004). Preparation and extraction of insoluble (inclusion-body) proteins from *Escherichia coli*. *Curr Protoc Protein Sci.* Chapter 6, Unit–6.3.
- Patel, S.** (2017). A critical review on serine protease: Key immune manipulator and pathology mediator. *Allergologia et immunopathologia* 45(6), 579–591.
- Pemberton, P. A., Stein, P. E., Pepys, M. B., Potter, J. M., and Carrell, R. W.** (1988). Hormone binding globulins undergo serpin conformational change in inflammation. *Nature* 336(6196), 257.
- Perner, J., Kropáčková, S., Kopáček, P., and Ribeiro, J. M. C.** (2018). Sialome diversity of ticks revealed by RNAseq of single tick salivary glands. *PLoS Negl Trop Dis.* 12(4), e0006410.
- Perner, J., Provazník, J., Schrenková, J., Urbanová, V., Ribeiro, J. M., and Kopáček, P.** (2016b). RNA-seq analyses of the midgut from blood- and serum-fed *Ixodes ricinus* ticks. *Sci Rep.* 6, 36695.
- Perner, J., Sobotka, R., Šíma, R., Konvičková, J., Sojka, D., Oliveira, P. L. D., et al.** (2016a). Acquisition of exogenous haem is essential for tick reproduction. *eLife.* 5, PMID:26949258
- Pettersen, E. F., Goddard, T. D., Huang, C. C., Couch, G. S., Greenblatt, D. M., Meng, E. C., and Ferrin, T. E.** (2004). UCSF Chimera--A visualization system for exploratory research and analysis. *J Comput Chem.* 25(13), 1605-12.
- Pham, T. N., Hayashi, K., Takano, R., Itoh, M., Eguchi, M., et al.** (1996) A new family of serine protease inhibitors (*Bombyx* family) as established from the unique topological relation between the positions of disulphide bridges and reactive site. *J Biochem.* 119, 428–434.
- Pirard, B.** (2007) Insight into the structural determinants for selective inhibition of matrix metalloproteinases. *Drug Discov. Today* 12, 640e646.
- Pospisilova, T., Urbanova, V., Hes, O., Kopacek, P., Hajdusek, O., and Sima, R.** (2019). Tracking of *Borrelia afzelii* transmission from infected *Ixodes ricinus* nymphs to mice. *Infect.*

Immun. 87, e00896-18.

Prevot, P. P., Adam, B., Boudjeltia, K. Z., et al. (2006). Antihemostatic effects of a serpin from the saliva of the tick, *Ixodes ricinus*. *J Biol Chem.* 281(36), 26361-26369.

Quinn, D. J., Weldon, S., and Taggart, C. C. (2010). Antiproteases as therapeutics to target inflammation in cystic fibrosis. *Open Respir. Med. J.* 4, 20–31.

Ra, H. J., and Parks, W. C. (2007). Control of matrix metalloproteinase catalytic activity. *Matrix Biol.* 26, 587e596.

Ramamoorthi, N., Narasimhan, S., Pal, U., Bao, F., Yang, X. F., Fish, D., Anguita, J., Norgard, M. V., Kantor, F. S., Anderson, J. F., Koski, R. A., and Fikrig, E. (2005). The Lyme disease agent exploits a tick protein to infect the mammalian host. *Nature* 436(7050), 573-7.

Ranasinghe, S., and McManus, D. P. (2013). Structure and function of invertebrate Kunitz serine protease inhibitors. *Dev. Comp. Immunol.* 39, 219–227.

Rawlings, N. D., Tolle, D. P., and Barrett, A. J. (2004). Evolutionary families of peptidase inhibitors. *Biochem. J.* 378, 705–716.

Ribeiro, J. M., Slovak, M., and Francischetti, I. M. (2017). An insight into the sialome of *Hyalomma excavatum*. *Ticks Tick Borne Dis.* 8, 201–207.

Rimphanitchayakit, V., and Tassanakajon, A. (2010). Structure and function of invertebrate Kazal-type serine proteinase inhibitors. *Dev. Comp. Immunol.* 34, 377–386.

Rosengren, K. J., Daly, N. L., Scanlon, M. J., and Craik, D. J. (2001). Solution structure of BSTI: A new trypsin inhibitor from skin secretions of *Bombina bombina*. *Biochemistry* 40(15), 4601-9.

Ruf, W. (2012). Tissue factor and cancer. *Thromb Res.* 130(Suppl 1), S84-S87.

Russell, R. A. L., Dryden, M. S., Pinto, A. A., and Lovett, J. K. (2018). Lyme disease: Diagnosis and management. *Pract Neurol.* 18(6), 455-464.

Sandhaus, R. A., and Turino, G. (2013). Neutrophil elastase-mediated lung disease. *COPD* 10 (Suppl. 1), 60–63.

- Sasaki, S. D., De Lima, C. A., Lovato, D. V., Juliano, M. A., Torquato, R. J., and Tanaka, A. S.** (2008). BmSI-7, a novel subtilisin inhibitor from *Boophilus microplus*, with activity toward Pr1 proteases from the fungus *Metarhizium anisopliae*. *Exp. Parasitol.* 118, 214–220.
- Schechter, M. E., Andrade, B. B., He, T., et al.** (2017). Inflammatory monocytes expressing tissue factor drive SIV and HIV coagulopathy. *Sci Transl Med.* 9(405), eaam5441.
- Schechter, I., and Berger, A.** (1967). On the size of the active site in proteases. I. Papain. *Biochem Biophys Res Commun.* 27(2), 157–162.
- Schlott, B., Wöhnert, J., Icke, C., Hartmann, M., Ramachandran, R., Gührs, K., H., Glusa, E., Flemming, J., Görlach, M., Große, F., and Ohlenschläger, O.** (2002). Interaction of Kazal-type inhibitor domains with serine proteinases: Biochemical and structural studies, *J. Mol. Biol.* 318(2), 533-546.
- Schwarz, A., von Reumont, B. M., Erhart, J., Chagas, A. C., Ribeiro, J. M., and Kotsyfakis, M.** (2013). *De novo Ixodes ricinus* salivary gland transcriptome analysis using two next-generation sequencing methodologies. *The FASEB Journal* 27(12), 4745–4756.
- Schwarz, A., Tenzer, S., Hackenberg, M., Erhart, J., Gerhold-Ay, A., Mazur, J., Kuharev, J., Ribeiro, J. M., and Kotsyfakis, M.** (2014). A systems level analysis reveals transcriptomic and proteomic complexity in *Ixodes ricinus* midgut and salivary glands during early attachment and feeding. *Mol Cell Proteomics.* 13(10), 2725-35.
- Scott, C. J., and Taggart, C C.** (2010). Biologic protease inhibitors as novel therapeutic agents. *Biochimie.* 92(11), 1681-1688.
- Silverman, G. A., Bird, P. I., Carrell, R. W., Coughlin, P. B., Gettins, P. G., Irving, J. I., and Remold-O'Donnell, E.** (2001). The serpins are an expanding superfamily of structurally similar but functionally diverse proteins: Evolution, mechanism of inhibition, novel functions, and a revised nomenclature. *J Biol Chem.* 276(36), 33293-33296.
- Soares, T. S., Oliveira, F., Torquato, R. J. S., Sasaki, S. D., Araujo, M. S., Paschoalin, T., et al.** (2016). BmTI-A, a Kunitz-type inhibitor from *Rhipicephalus microplus* able to interfere in vessel formation. *Vet. Parasitol.* 219, 44–52.

- Somprasong, N., Rimphanitchayakit, V., and Tassanakajon, A.** (2006). A five domain Kazal-type serine proteinase inhibitor from black tiger shrimp *Penaeus monodon* and its inhibitory activities. *Dev. Comp. Immun.* 30, 998–1008.
- Sonenshine, D. E., and Anderson, J.** (2014). Mouthparts and digestive system, in *Biology of Ticks*, 2nd Edn., eds. Sonenshine, D. E., and Michael, R. NY: *Oxford University Press*. 122–162.
- Soualmia, F., and El Amri, C.** (2017). Serine protease inhibitors to treat inflammation: A patent review (2011-2016). *Expert Opinion on Therapeutic Patents, Informa Healthcare*, 28(2), 93-110.
- Stassens, P., Bergum, P. W., Gansemans, Y., Jespers, L., Laroche, Y., Huang, S., et al.** (1996). Anticoagulant repertoire of the hookworm *Ancylostoma caninum*. *Proc. Natl. Acad. Sci. U.S.A.* 93, 2149–2154.
- Steinegger, M., Meier, M., Mirdita, M., Vöhringer, H., Haunsberger, S. J., and Söding, J.** (2019). HH-suite3 for fast remote homology detection and deep protein annotation. *BMC Bioinformatics* 20, 473.
- Studer, G., Rempfer, C., Waterhouse, A.M., Gumienny, G., Haas, J., Schwede, T.** (2020). QMEANDisCo - Distance constraints applied on model quality estimation. *Bioinformatics* 36, 1765-1771.
- Swanson, S. J., Neitzel, D., Reed, K. D., and Belongia, E. A.** (2006). Coinfections acquired from *Ixodes* ticks. *Clin. Microbiol. Rev.* 19, 708–727.
- Tamura, K., and Nei, M.** (1993). Estimation of the number of nucleotide substitutions in the control region of mitochondrial DNA in humans and chimpanzees. *Molecular Biology and Evolution* 10, 512-526.
- Tang, H., Kambris, Z., Lemaitre, B., and Hashimoto, C.** (2008). A serpin that regulates immune melanization in the respiratory system of *Drosophila*. *Dev Cell.* 15, 617-26.
- Tirloni, L., Islam, M. S., Kim, T. K., Diedrich, J. K., Yates, J. R. III, Pinto, A. F., et al.** (2015). Saliva from nymph and adult females of *Haemaphysalis longicornis*: A proteomic study. *Parasit. Vectors* 8, 338.

- Tirloni, L., Kim, T. K., Pinto, A. F. M., Yates, J. R. III, Da Silva Vaz, I. Jr., et al.** (2017). Tick-host range adaptation: Changes in protein profiles in unfed adult *Ixodes scapularis* and *Amblyomma americanum* saliva stimulated to feed on different hosts. *Front. Cell Infect. Microbiol.* 7, 517.
- Tirloni, L., Reck, J., Terra, R. M., Martins, J. R., Mulenga, A., Sherman, N. E., et al.** (2014). Proteomic analysis of cattle tick *Rhipicephalus (Boophilus) microplus* saliva: A comparison between partially and fully engorged females. *PLoS One* 9, e94831.
- Travis, J., Potempa, J., and Maeda, H.** (1995). Are bacterial proteinases pathogenic factors? *Trends Microbiol.* 3, 405e407.
- Tripathi, L. P., and Sowdhamini, R.** (2008). Genome-wide survey of prokaryotic serine proteases: Analysis of distribution and domain architectures of five serine protease families in prokaryotes. *BMC Genomics* 9:549.
- Turk, B.** (2006). Targeting proteases: Successes, failures and future prospects. *Nat Rev Drug Discov.* 5(9), 785–799.
- Umezawa, H., Aoyagi, T., Morishima, H., Matsuzaki, M., and Hamada, M.** (1970). Pepstatin, a new pepsin inhibitor produced by Actinomycetes. *J. Antibiot.* 23(5), 259–62.
- Vergnolle, N.** (2016). Protease inhibition as new therapeutic strategy for GI diseases. *Gut* 65(7), 1215–1224.
- Versteeg, H. H., Schaffner, F., Kerver, M., et al.** (2008). Inhibition of tissue factor signaling suppresses tumor growth. *Blood* 111(1), 190-199.
- Wan, H., Lee, K. S., Kim, B. Y., Zou, F. M., Yoon, H. J., and Je, Y. H.** (2013). A spider-derived Kunitz-type serine protease inhibitor that acts as a plasmin inhibitor and an elastase inhibitor. *PLoS ONE* 8:e53343.
- Wang, Y. W., Tan, J. M., Du, C. W., Yan, X. W., Lai, R., and Lu, Q. M.** (2015). A novel trypsin inhibitor-like cysteine-rich peptide from the frog *Lepidobatrachus laevis* containing proteinase-inhibiting activity. *Nat. Prod. Bioprospect.* 5, 209–214.

Wang, Z. H., Zhao, X. F., and Wang, J. X. (2009). Characterization, kinetics, and possible function of Kazal-type proteinase inhibitors of Chinese white shrimp, *Fenneropenaeus chinensis*. *Fish Shellfish Immunol.* 26, 885–897.

Waterhouse, A., Bertoni, M., Bienert, S., Studer, G., Tauriello, G., Gumienny, R., Heer, F.T., de Beer, T.A.P., Rempfer, C., Bordoli, L., Lepore, R., and Schwede, T. (2018). SWISS-MODEL: Homology modelling of protein structures and complexes. *Nucleic Acids Res.* 46(W1), W296-W303.

Waxler, B., and Rabito, S. F. (2003). Aprotinin: A serine protease inhibitor with therapeutic actions: Its interaction with ACE inhibitors. *Curr. Pharm. Des.* 9, 777e787.

Wingfield, P. T. (2015). Overview of the purification of recombinant proteins. *Curr Protoc Protein Sci.* 80, 6.1.1-6.1.35.

Wingfield, P. T., Stahl, S.J., Kaufman, J., Zlotnick, A., Hyde, C. C., Gronenborn, A.M., and Clore, G. M. (1997). The extracellular domain of immunodeficiency virus gp41 protein: expression in *Escherichia coli*, purification, and crystallization. *Protein Sci.* 6(8), 1653-60.

Wu, S., and Zhang, Y. (2007). LOMETS: A local meta-threading-server for protein structure prediction. *Nucleic Acids Res.* 35, 3375-3382.

Yan, Y., Orcutt, S., and Strickler, J. (2009). The use of SUMO as a fusion system for protein expression and purification. *Chem Today* 27, 42–47.

Yang, L., Lee, K. S., Kim, B. Y., Choi, Y. S., Yoon, H., J., Jia, J., and Jin, B. R. (2017). Anti-fibrinolytic and anti-microbial activities of a serine protease inhibitor from honeybee (*Apis cerana*) venom. *Comp. Biochem. Phys.Part C: Toxicology & Pharmacology* 201, 11-18.

Zeng, X. C., Liu, Y., Shi, W., Zhang, L., Luo, X., Nie, Y and Yang, Y. (2014). Genome-wide search and comparative genomic analysis of the trypsin inhibitor-like cysteine-rich domain-containing peptides. *Peptides* 53, 106-114.

- Zhao, P., Dong, Z., Duan, J., Wang, G., Wang, L., Li, Y. et al.** (2012). Genome-wide identification and immune response analysis of serine protease inhibitor genes in the silkworm, *Bombyx mori*. *PLoS ONE* 7, e31168.
- Zheng, S., Wang, H., and Zhang, G.** (2011). A novel alkaline protease from wild edible mushroom *Termitomyces albuminosus*. *Acta Biochim Pol.* 58, 269–273.
- Zheng, W., Zhang, C., Wuyun, Q., Pearce, R., Li, Y., and Zhang, Y.** (2019). LOMETS2: Improved meta-threading server for fold-recognition and structure-based function annotation for distant-homology proteins. *Nucleic Acids Res.*, 47(W1), W429-W436.
- Zhu, Y., Underwood, J., Macmillan, D., et al.** (2017). Persistent kallikrein 5 activation induces atopic dermatitis-like skin architecture independent of PAR2 activity. *J Allergy Clin Immunol.* 140, 1310–1322.
- Zou, Z., Anisowicz, A., Hendrix, M. J., Thor, A., Neveu, M., Sheng, S., and Sager, R.** (1994). Maspin, a serpin with tumor-suppressing activity in human mammary epithelial cells. *Science* 263(5146), 526-529.

8 Supplement

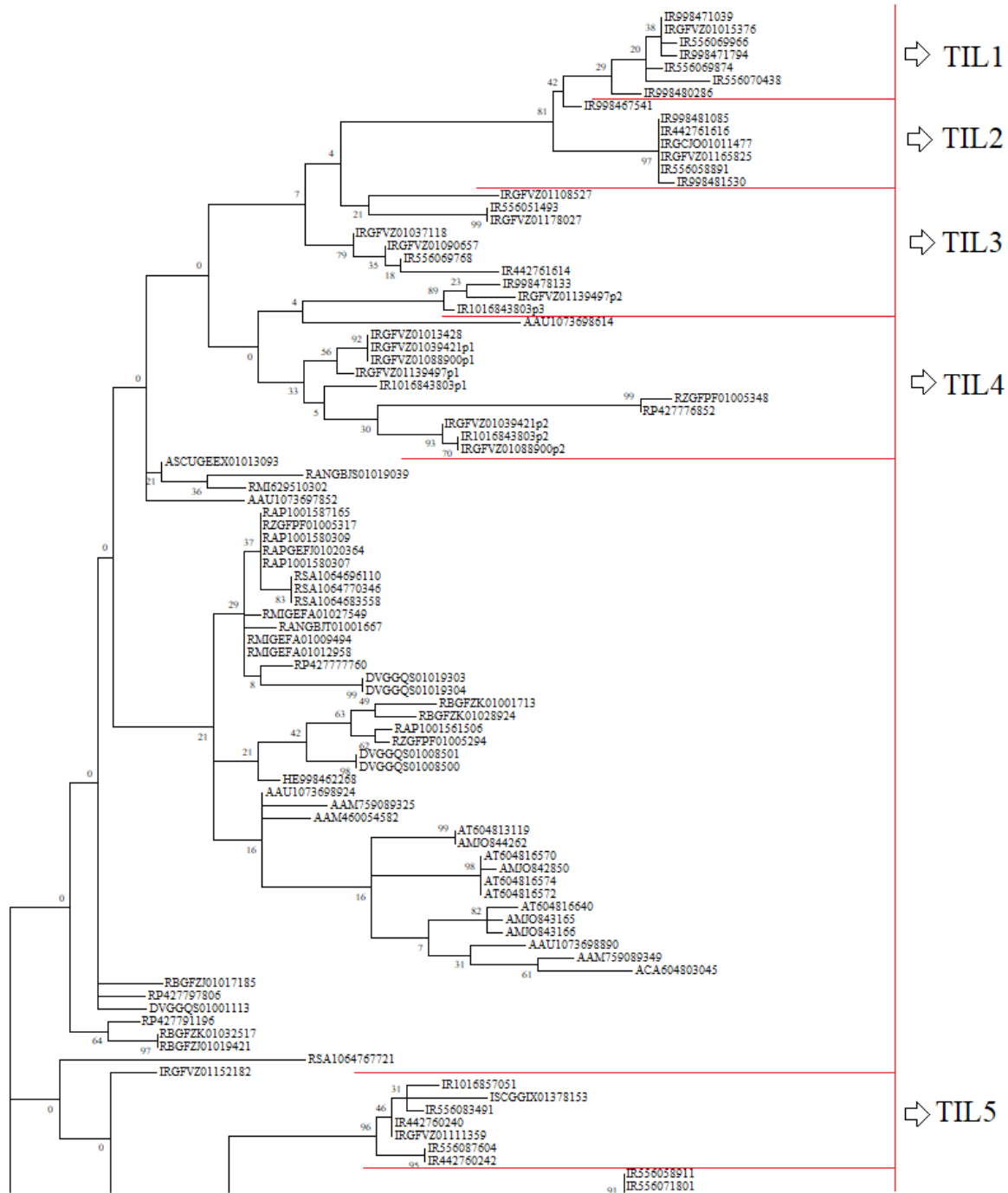
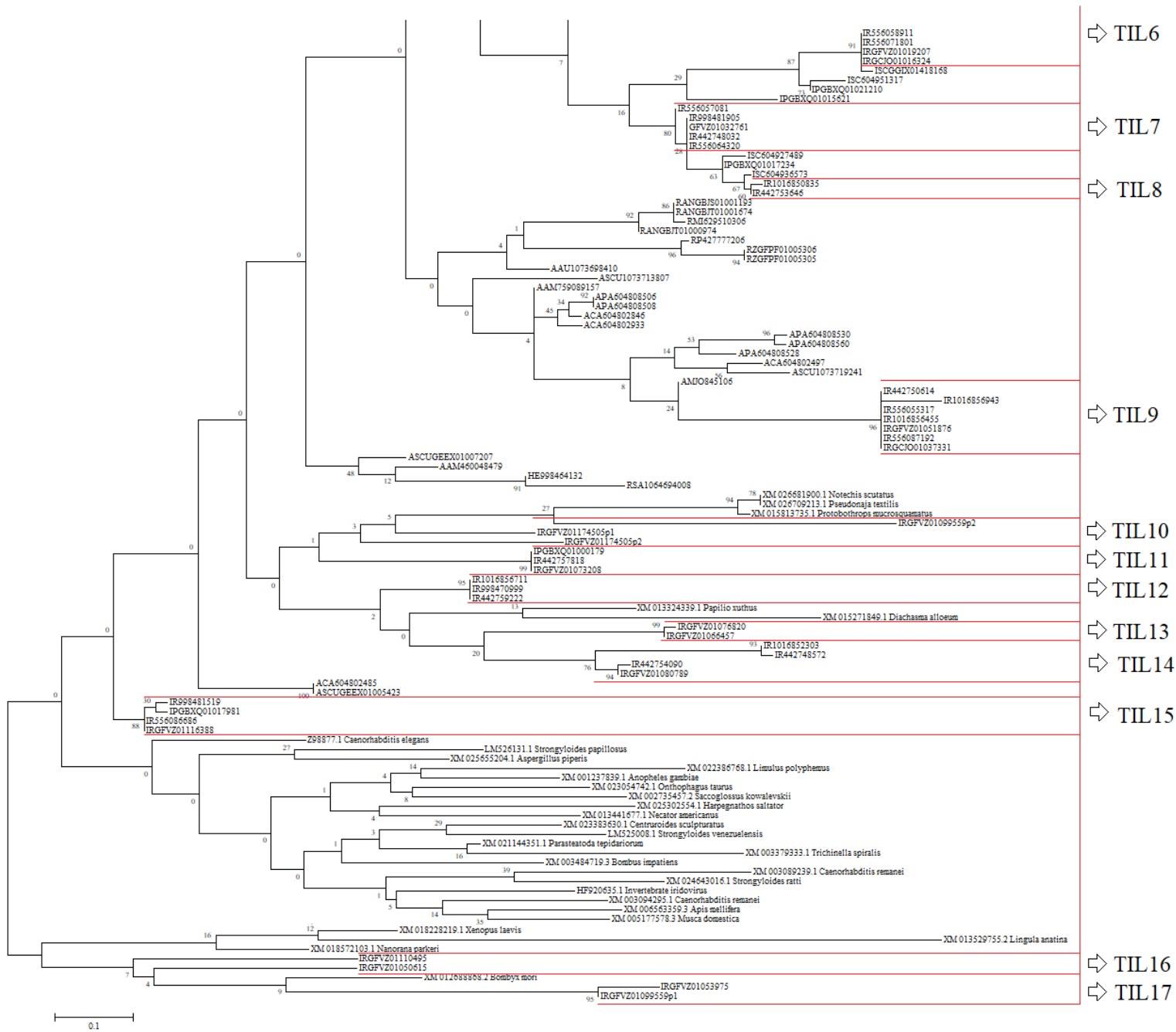


Figure S1: Maximum Likelihood (ML) phylogenetic tree of TIL-domain inhibitors from *I. ricinus*, Ixodida and other non-Ixodida species. The individual clusters were designated as TIL-1-17 protein groups. The numbers next to the branches represent percentage in which associated taxa cluster together.



Continued Figure S1: Maximum Likelihood (ML) phylogenetic tree of TIL-domain inhibitors from *I. ricinus*, Ixodida and other non-Ixodida species. The individual clusters were designated as TIL-1-17 protein groups. The numbers next to the branches represent percentage in which associated taxa cluster together.